1953

Studies of the Kinetics of Electrode Processes.

George Louis Stiehl
Louisiana State University and Agricultural & Mechanical College

STUDIES OF THE KINETICS OF ELECTRODE PROCESSES

A Dissertation

Submitted to the Graduate Faculty of the
Louisiana State University and
Agricultural and Mechanical College
in partial fulfillment of the
requirements for the degree of
Doctor of Philosophy

in

The Department of Chemistry

by
George Louis Stiehl, Jr.
B. S., Oklahoma City University, 1949
M. S., Louisiana State University, 1951
June, 1953

ProQuest LLC.
789 East Eisenhower Parkway
P.O. Box 1346
Ann Arbor, MI 48106 - 1346

MANUSCRIPT THESES

Unpublished theses submitted for the master's and doctor's degrees and deposited in the Louisiana State University Library are available for inspection. Use of any thesis is limited by the rights of the author. Bibliographical references may be noted, but passages may not be copied unless the author has given permission. Credit must be given in subsequent written or published work.

A library which borrows this thesis for use by its clientele is expected to make sure that the borrower is aware of the above restrictions.

LOUISIANA STATE UNIVERSITY LIBRARY

ACKNOWLEDGMENT

The writer is greatly appreciative of the guidance given him by Dr. Paul Delahay, who directed the planning and the execution of these investigations. He wishes to express his thanks to the members of his advisory committee, Dr. W. R. Edwards and Dr. Stanley Bashkin, for their patient consideration of the manuscript. He wishes to acknowledge the work of Mr. Wilbur B. Payne and Mr. Theodore E. Leinhardt, who constructed the "Potentiostats" and the pH control units described in Chapter VI. Credit is due Mr. Bernie Holmes for the photograph used in Figure 8. To his wife, Mrs. Jo Ann Stiehl, and to Mary Effie Smith, for their typing, the writer is also most grateful.

The work embodied in this dissertation was sponsored by the Office of Naval Research under the form of a fellowship. The candidate is grateful to this organization for financial support.

TABLE OF CONTENTS

LIST OF FIGURES

LIST OF TABLES

ABSTRACT

Part I

In this dissertation a theoretical treatment is developed for polarographic currents controlled by diffusion and by the rate of a catalytic process which regenerates the substance reacting at the dropping mercury electrode. The properties of catalytic currents are treated and a graphical method for the determination of rate constants from experimental currents is reported. The theory is applied to the catalytic currents observed in the reduction of ferric ion in presence of hydrogen peroxide. Calculated and experimental rate constants are in good agreement and also agree well with reported rate constants as obtained by a chemical method.

Part II

General criteria for the experimental study of the anodic oxidation of metals are established, and it is shown that reliable results can be obtained when the potential of the metal undergoing oxidation, and the pH of the electrolyte are controlled automatically during electrolysis. An approximate treatment is developed for the kinetics of the electrolytic oxidation of metals at constant potentials in stirred solution, and this treatment is verified experimentally. Optimum experimental conditions are deduced from theoretical principles. Experimental methods are briefly outlined; the potential of the metal is controlled by means

of a potentiostat, and the pH of the electrolyte is maintained at a constant value by the addition of acid or base to the solution. All controls are made automatically by suitable electronic devices. Examples of curves showing the variations of the rate of oxidation with potential at constant pH are presented for iron, and the complete investigation is summarized in a potential-pH diagram showing lines of equal rates of oxidation. Such diagrams are presented for iron, tin, and lead. The features of these diagrams are explained on the basis of thermodynamic potential-pH diagrams for these metals, and the discrepancies between equilibrium and experimental diagrams are interpreted.

INTRODUCTION

This dissertation is divided into two parts which are not directly related, and consequently, introductory remarks and reviews of the literature will be given in each part separately.

PART I

THEORY OF CATALYTIC POLAROGRAPHIC CURRENTS

CHAPTER I

INTRODUCTION AND REVIEW OF THE LITERATURE

In previous work done at Louisiana State University (1, 11, 12, 17, 43) the theory of polarographic currents controlled by diffusion and by the rate of an heterogeneous reaction was developed and applied to various electrode processes. This theory is applicable to cases in which the chemical process, partially controlling the current, occurs essentially at the surface of the electrode. This condition is fulfilled in the case of so-called irreversible waves, but there are cases in which the current is controlled by diffusion and by a reaction occurring at the surface of the electrode and in the "vicinity" of the electrode. The theory of these so-called "catalytic" currents is developed in this dissertation for cases in which the regeneration process is a first-order reaction. The justification for the rather unexpected use of the term "catalytic" will become apparent in the course of the subsequent discussion.

The nature of catalytic polarographic currents can be explained by considering an electrode process in which a substance O is reduced to another substance R at the dropping mercury electrode (reaction (1)). The solution also contains a substance Z which is not reduced at the dropping mercury electrode at the potential at which the limiting current for O is observed.

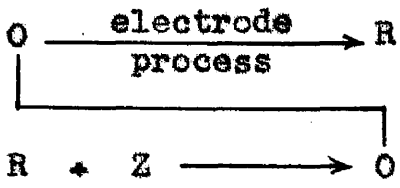

Furthermore, Z reacts with R to regenerate substance O (reaction (2)). Because of this effect of substance Z, the limiting current corresponding to reaction (1) is increased when Z is present in solution. The increase in current is determined by the kinetics of reaction (2) and by the diffusion processes of substance O, R, and Z. Various catalytic waves of this type have been reported. Hydrogen peroxide causes a large increase in the limiting currents of ferric ion, and of peroxy-compounds of molybdenum, tungsten and vanadium (26). Proteins containing a sulfhydryl group yield catalytic waves which have been explained by a mechanism involving reactions of the type represented by equations (1) and (2) (See reference (25)). Finally, various alkaloids are known to give catalytic waves which can be explained similarly (24).

In a slightly different type of catalytic wave, substance R produced in the electrode process (equation (1)) reacts with Z to give a substance P which is not reduced at the potential at which the limiting current of O is observed. Under these conditions the limiting current for reaction (1) is not affected by the formation of P, but the latter substance may in some cases yield a wave at more negative potentials. Catalytic waves of this type have been observed in the

reduction of oxygen in presence of various substances such as hemoglobin (4) and carbonic acid (44).

The only theoretical treatment of catalytic polarographic currents reported prior to the publication of the material contained in this dissertation was the one developed by Brdicka and Wiesner (5). The theory proposed by these authors does not take into account quantitatively the diffusion phenomena occurring at the dropping mercury electrode. As a result, rate constants for reaction (2) one calculates on the basis of this theory are about 10^4 too high as pointed out by Kolthoff and Parry (26). Other features of catalytic waves such as the decrease in current resulting from an increase in the head of mercury also cannot be explained on the basis of the theory of Brdicka and Wiesner. A more rigorous treatment accounting quantitatively for the properties of catalytic currents is reported in the present dissertation. The theory is developed for catalytic currents of the type described by reactions (1) and (2), but the treatment is also applicable to the case in which a new wave results from the catalytic process (substance P mentioned above). One month after the publication of this work, Miller (35) reported a treatment based on the same ideas as these expressed. The mathematical approach was, however, slightly different.

CHAPTER II

THEORETICAL TREATMENT

CASE OF LINEAR DIFFUSION

The Boundary Value Problem

Consider a plane electrode at which a substance O is reduced to substance R by a process which is assumed to be instantaneous (reaction (1) See page 2, Chapter I). The change of concentration between two planes at the distance x and x + dx from the electrode is the sum of the following two terms: (1) the difference in the flux of substance O at x and x + dx; (2) the change in concentration caused by regeneration of substance O by reaction (2). The first term is calculated in the theory of linear diffusion[1], and is equal to the product of $\partial^2 C_O / \partial x^2$ by the diffusion coefficient D_O of substance O. The second term which depends on the kinetics of reaction (2) is

$$\frac{\partial C_o(x,t)}{\partial t} = k_f C_R(x,t)\ C_z\ (x,t) - k_b C_o\ (x,t) \qquad (3)$$

where k_f and k_b are formal rate constants for reaction (2), and the C's are the concentrations, which are functions of x and t. Where t is the time elapsed from the beginning of

---

[1] See reference (25), page 18.

the electrolysis. From the foregoing considerations one deduces that the following differential equation should be obeyed

$$\frac{\partial C_O(x,t)}{\partial t} = D_O \frac{\partial^2 C_O(x,t)}{\partial x^2} + k_f C_R(x,t) C_Z(x,t) - k_b C_O(x,t) \qquad (4)$$

Likewise one can write for substance R

$$\frac{\partial C_R(x,t)}{\partial t} = D_R \frac{\partial^2 C_R(x,t)}{\partial x^2} - k_f C_R(x,t) C_Z(x,t) + k_b C_O(x,t) \qquad (5)$$

Two simplifications will now be introduced by assuming: (1) that the effect of the backward process in reaction (2) can be neglected; (2) that there is a large excess of substance Z, so that the concentration $C_Z(x,t)$ can be equated to the bulk concentration C_Z^o of substance Z. The system of equations (4) and (5) can then be written in the simplified form

$$\frac{\partial C_O(x,t)}{\partial t} = D_O \frac{\partial^2 C_O(x,t)}{\partial x^2} + k_f C_Z^o C_R(x,t) \qquad (6)$$

$$\frac{\partial C_R(x,t)}{\partial t} = D_R \frac{\partial^2 C_R(x,t)}{\partial x^2} - k_f C_Z^o C_R(x,t) \qquad (7)$$

One boundary condition was obtained by expressing that the sum of the fluxes of substances O and R is equal to zero at the electrode surface. Hence

$$D_O \left(\frac{\partial C_O(x,t)}{\partial x}\right)_{x=0} + D_R \left(\frac{\partial C_R(x,t)}{\partial x}\right)_{x=0} = 0 \qquad (8)$$

The second boundary condition can be readily derived by assuming that the concentration of substance O at the electrode surface is equal to zero during electrolysis. This implies that the rate of reaction (1) is much larger than the rate of the process being considered here. Such a hypothesis is justified since the rate of the reaction can be made very large by adjusting the electrode potential at a sufficiently cathodic value. Thus

$$C_O\ (0,t) = 0 \tag{9}$$

The initial conditions can be prescribed at will, for example

$$C_O\ (x,0) = C^o \tag{10}$$

and

$$C_R\ (x,0) = 0 \tag{11}$$

By writing equation (10) it is assumed that the distribution of substance O is uniform in solution before electrolysis. Equation (11) simply expresses that substance R is not present in solution at any appreciable concentration before electrolysis.

Derivation of the concentration $C_O\ (x,t)$.

The above boundary value problem will now be solved by applying the Laplace transformation (8), but before doing so it is advantageous to note that concentrations O and R are related by the very simple relationship

$$C_R\ (x,t) = C^\circ - C_o\ (x,t) \tag{12}$$

which is written on the assumption that the diffusion coefficients D_O and D_R are equal. This assumption is justified because substances O and R have in general approximately the same size. Equation (12) results directly from equation (8) and Duhamel's theorem (6).

In view of equation (12), the differential equation (6) can now be written

$$\frac{\partial C_0(x,t)}{\partial t} = D \frac{\partial^2 C_0(x,t)}{\partial x^2} + k_f C_z^\circ \left[C^\circ - C_0(x,t)\right] \tag{13}$$

when D is the common value of D_O and D_R. The latter equation can be rewritten by introducing the function

$$u(x,t) = C^\circ - C_0(x,t) \tag{14}$$

Thus:

$$\frac{\partial u(x,t)}{\partial t} = D \frac{\partial^2 u(x,t)}{\partial x^2} - k_f C_z^\circ u(x,t) \tag{15}$$

The corresponding Laplace transformation with respect to t is

$$\frac{d^2 \bar{u}(x,s)}{dx^2} - \frac{s + k_f C_z^\circ}{D} \bar{u}(x,s) = 0 \tag{16}$$

The solution of the above differential equation is

$$\bar{u}(x,s) = \xi \exp\left[-x\left(\frac{s + k_f C_z^\circ}{D}\right)^{1/2}\right] \tag{17}$$

where ξ is an integration constant to be determined by the boundary condition $C_0\ (0,t) = 0$ (i.e. by the condition $\bar{u}(0,s) = C^\circ/s$. By inverse transformation of the equation (17) in which $\xi = C^\circ/s$, one obtains the function $u(x,t)$ and consequently, the concentration $C_0\ (x,t)$. Thus

$$C_0 = C^\circ \left\{ \begin{array}{l} 1 - \tfrac{1}{2} \exp\left[-x\left(\frac{k_f C_2^\circ}{D_0}\right)^{1/2}\right] \operatorname{erfc}\left[\frac{x}{2(D_0 t)^{1/2}} - (k_f C_2^\circ t)^{1/2}\right] \\ -\tfrac{1}{2} \exp\left[x\left(\frac{k_f C_2^\circ}{D_0}\right)^{1/2}\right] \operatorname{erfc}\left[\frac{x}{2(D_0 t)^{1/2}} + (k_f C_2^\circ t)^{1/2}\right] \end{array} \right\} \qquad (18)$$

in which the notation erfc (ψ) represents the complement of the error function as defined by

$$\operatorname{erfc}(\psi) = 1 - \frac{2}{\pi^{1/2}} \int_0^{\psi} \exp(-z^2)\, dz \qquad (19)$$

The value of $C_0\ (x,t)$ from equation (18) was plotted against x in Figure 1 for the following data: $C^\circ = 10^{-5}$ mole per cm.^{3}, $D_0 = 10^{-5}$ cm.^{2} sec.$^{-1}$, $C_2 = 10^{-3}$ mole per cm.^{3}, $t = 10$ sec. The various curves correspond to values of the rate constant k_f from 0 to 1000 sec.$^{-1}$ (moles per cm.^{3})$^{-1}$. This diagram shows that the decrease of concentration C_0 is less pronounced when there is regeneration by reaction (2). When k_f is smaller than 10 sec.$^{-1}$ (moles per cm.^{3})$^{-1}$, the catalytic effect is negligible after 10 seconds.

By introducing $k_f = 0$ in equation (18) it can be seen that the resulting value of C_0 is identical with that

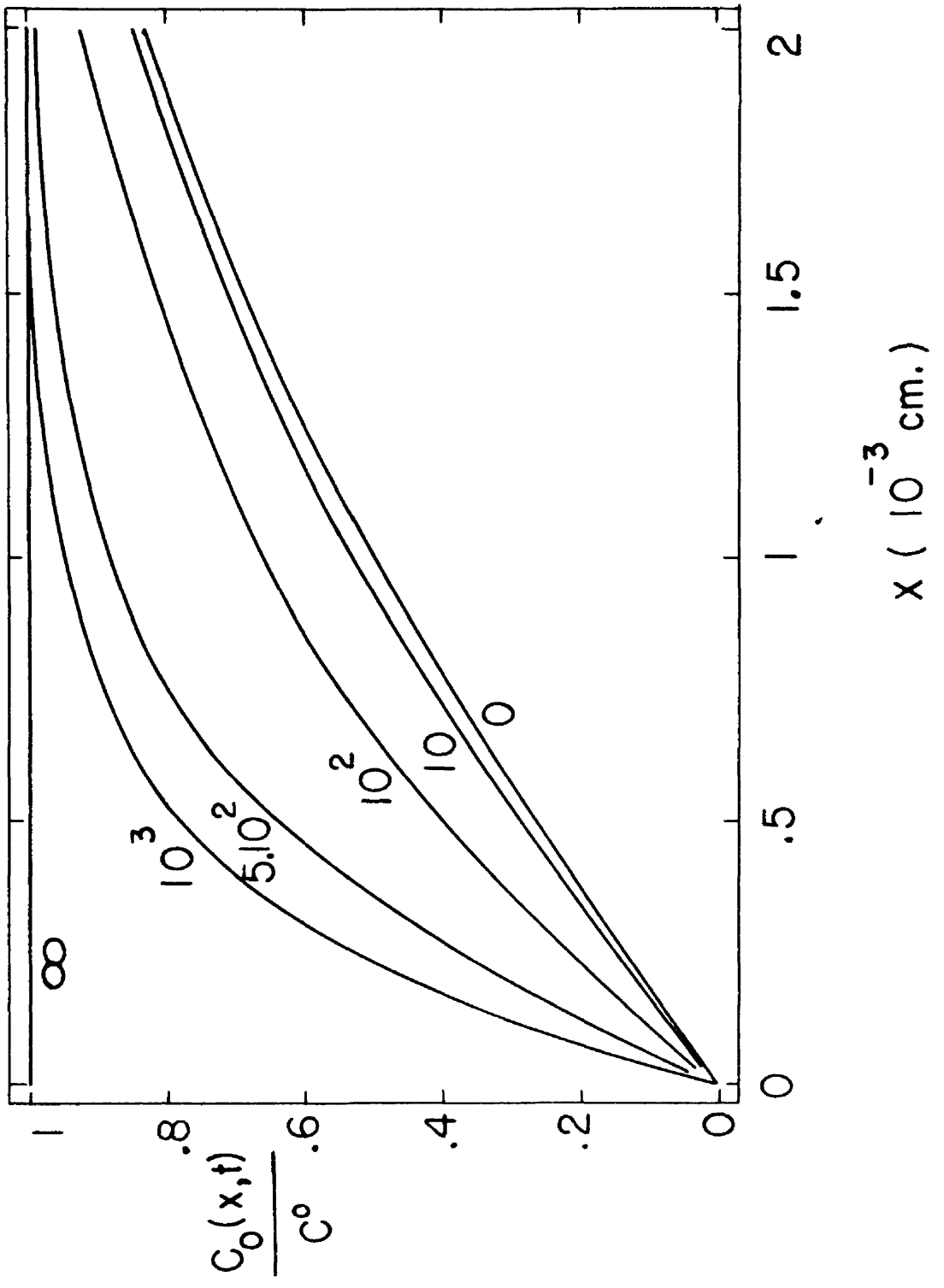

Figure 1. Variations of concentration C_o with the distance from the electrode. Number on each curve is the value of rate constant k_f in sec.$^{-1}$ (moles per cm.3)$^{-1}$.

obtained in the theory of simple linear diffusion. This is to be expected since there is no catalytic effect. On the other hand, when k_f is infinite, one obtains $C_0 = C^o$ after expanding (38) the error integrals in equation (18). This is to be expected since for $k_f = \infty$, substance O is regenerated as soon as it is consumed.

Variations of Current

The current is obtained by multiplying the flux at the electrode surface by the charge involved in the reduction of one mole of substance O. The flux is the product of the diffusion coefficient D_0 divided by the gradient of concentration $(\partial C_0(x,t)/\partial x)_{x=0}$ which is obtained by differentiating equation (18) with regard to x and introducing x = 0 in the resulting equation. Noticing that erf $(-\psi) = -$erf (ψ) one obtains after a simple transformation.

$$i = nFA D_0^{1/2} C^o \left\{ (k_f C_z^o)^{1/2} erf\left[(k_f C_z^o t)^{1/2}\right] + \frac{exp(-k_f C_z^o t)}{(\pi t)^{1/2}} \right\} \quad (20)$$

in which n is the number of electrons involved in the electrode process, F the Faraday, A the area of the electrode in cm^2, and the notation erf (ψ) represents the error integral

$$erf(\psi) = \frac{2}{\pi^{1/2}} \int_0^{\psi} exp(-z^2) dz \quad (21)$$

When $k_f = 0$, equation (20) is identical with the equation for a current controlled by simple linear diffusion[2]. When $k_f = \infty$ equation (20) yields an infinite current. This is to be expected since it was assumed that concentration C_Z^o at the surface of the electrode is the same as in the bulk of the solution. Actually for $k_f = \infty$, one should take into account the decrease in C_Z^o at the surface of the electrode, but this decrease was neglected in the present treatment.

As an example, the current i given by (20) is plotted against time in Figure 2 for the following data: $n = 1$, $A = 1$ cm.^{2}, $D_O = 10^{-5}$ cm.^{2} sec.$^{-1}$, $C^o = 10^{-5}$ moles cm^{-3}, $C_Z^o = 10^{-3}$ moles cm^{-3}; and for values of k_f from 0 to 1000 sec.$^{-1}$ (moles per cm^3)$^{-1}$. Figure 2 shows that because of the catalytic effect the current decreases less rapidly than in the case of simple diffusion. In the present case, the catalytic effect is noticeable when k_f is larger than 10 sec.$^{-1}$ (moles per cm^3)$^{-1}$.

CASE OF THE DROPPING MERCURY ELECTRODE

Instantaneous Total Current

In principle, catalytic polarographic currents could be calculated by following the method applied in the previous section and by using the corresponding equations for diffusion of an expanding sphere. However, the mathematical treatment would be arduous, and it is much simpler to apply the following method. When the rate constant k_f is equal

---

[2] See reference (25), page 18.

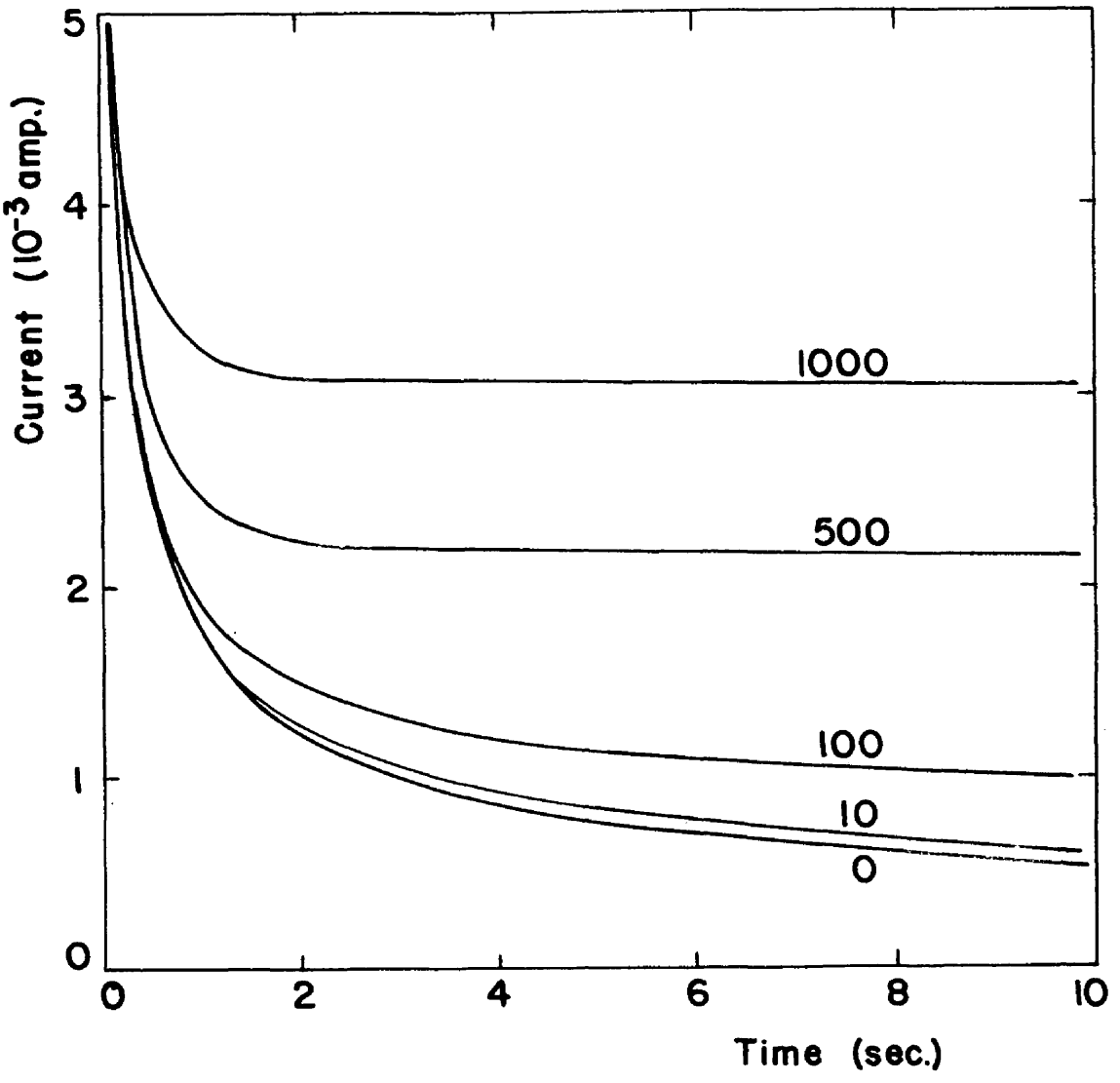

Figure 2. Variations of current (equation (20)) with time. Number on each curve is the value of rate constant k_f in sec.$^{-1}$ (moles per cm.3)$^{-1}$.

to zero, equation (20) is identical to the Ilkovic equation provided that the righthand side of equation (20) be multiplied by $(7/3)^{1/2}$. This is the factor which was used by Ilkovic to adjust the results of linear diffusion to the case of the dropping mercury electrode (23). By using the same factor in the case of a rate constant different from zero, and replacing the area A by its value calculated in terms of the characteristics of the capillary, one obtains after numerical transformations

$$i_t = 1.255 \times 10^6 n m^{2/3} t^{2/3} D_0^{1/2} C^0 \left\{ (k_f C_Z^0)^{1/2} \operatorname{erf}\left[(k_f C_Z^0 t)\right] + \frac{\exp(-k_f C_Z^0 t)}{(\pi t)^{1/2}} \right\} \qquad (22)$$

in which i_t is in microamperes, m is the rate of flow of mercury in mg. $sec.^{-1}$, t the time in sec. of the drop life at which the current is measured, D_0 the diffusion coefficient in cm^2 $sec.^{-1}$, k_f the rate constant in $sec.^{-1}$ (moles per liter)$^{-1}$ for the forward reaction (2), and C^0 and C_Z^0 the concentrations of O and Z in moles per liter. It should be pointed out that equation (22) is approximate on account of the introduction of the correction factor $(7/3)^{1/2}$.

Separation of Diffusion and Catalytic Currents

It is interesting for further discussion to separate the current given by equation (22) into the catalytic current due to reaction (2) and the limiting current which is observed when substance Z is not present. By subtracting the latter current as given by the Ilkovic equation from equation (22) one obtains the instantaneous catalytic current i_c.

Thus

$$i_c = 1.255\times10^6\, n m^{2/3} t^{2/3} D_o^{1/2} C^o \left\{ (k_f C_z^o)^{1/2} \operatorname{erf}\left[(k_f C_z^o t)^{1/2}\right] - \frac{1-\exp(-k_f C_z^o t)}{(\pi t)^{1/2}} \right\} \qquad (23)$$

in which the units are the same as in equation (22).

Average Catalytic Current and Determination of k_f from Experimental Currents

The average catalytic current during the drop life can be written in the abridged form.

$$(i_c)_{dv} = 1.255\times10^6\, \sigma\, n m^{2/3} D_o^{1/2} C^o \qquad (24)$$

in which the function σ is defined by

$$\sigma = (k_f C_z^o)^{1/2} \frac{1}{\tau} \int_0^\tau t^{2/3} \operatorname{erf}\left[(k_f C_z^o t)^{1/2}\right] dt - \frac{1}{\tau \pi^{1/2}} \int_0^\tau t^{1/6} \left[1-\exp(-k_f C_z^o t)\right] dt \qquad (25)$$

Values of function σ were calculated for drop times from 1 to 5 sec., and for values of $k_f C_z^o$ from 0.01 to 100 $sec.^{-1}$. The results are plotted in Figure 3. The principle of the calculation of σ is as follows: the functions under the integral sign in equation (25) were plotted against t, and the values of the integrals of equation (25) were obtained by graphic integration for different values of τ and $k_f C_z^o$.

The rate constant k_f is calculated from an experimental current in the following manner. First, the value of σ is

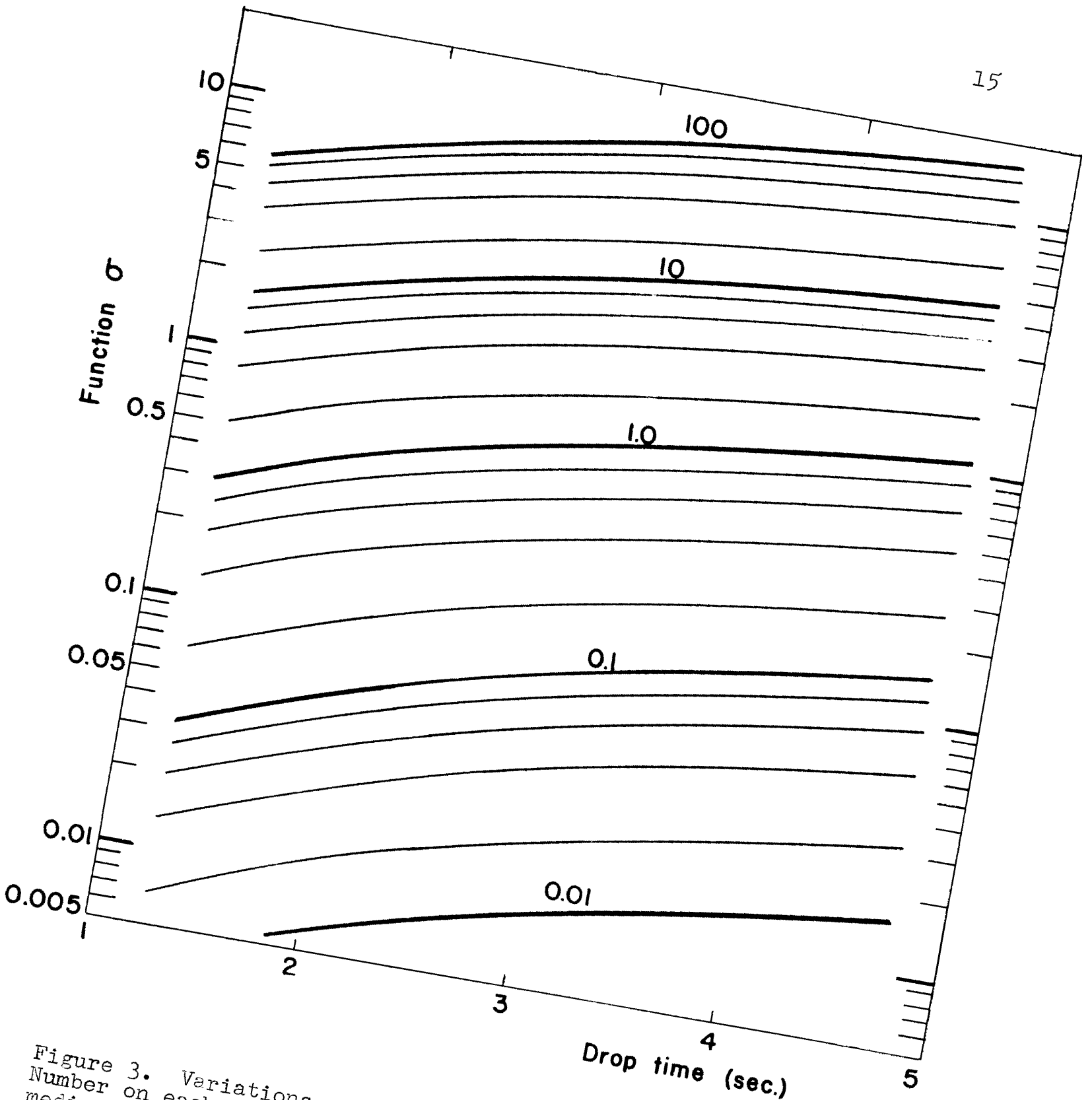

Figure 3. Variations of σ (equation (18)) with drop time τ. Number on each curve is the value of $k_f C_Z^o$ in sec.$^{-1}$. Intermediate curves correspond to values of $k_f C_Z^o$ which are multiple or submultiple of 2, 4, 6, 8.

obtained from the experimental current by application of equation (24); and the point having the corresponding coordinates σ and ζ is located on Figure 3. The value of $k_f C_z^o$ for the curve passing through this point is determined by interpolation, and the rate constant is calculated from the value of $k_f C_z^o$ thus obtained.

When $k_f C_z^o$ is larger than 100 sec.$^{-1}$, erf $\left[(k_f C_z^o t)^{1/2}\right]$ is practically equal to unity even for values of t as small as 0.15 seconds. Furthermore, the term exp $(-k_f C_z^o t)$ in equation (25) is virtually equal to zero when $k_f C_z^o$ is larger than 100. As a result, equation (25) is greatly simplified and the integration can be performed. Thus for $k_f C_z^o \gg 100$ sec.$^{-1}$

$$\sigma \cong \tfrac{3}{5} (k_f C_z^o)^{1/2} \zeta^{2/3} - \frac{6}{7\pi^{1/2}} \zeta^{1/6} \qquad (26)$$

and $k_f C_z^o$ is directly calculable from equations (24) and (26). Note that the second term on the right-hand side is much smaller than the first term. Therefore, the catalytic current is almost equal to the total current. Thus when $k_f C_z^o$ is larger than 100 sec.$^{-1}$, an approximate value of k_f can be obtained from the total current given by equation (22). The latter equation takes then the simplified form

$$(i_c)_{av} \cong (i_t)_{av} \cong \tfrac{3}{5}\, 1.255 \times 10^6\, n m^{2/3} \zeta^{2/3} D_o^{1/2} C^o C_z^{o\,1/2} k_f^{1/2} \qquad (27)$$

which yields directly the rate constant k_f.

PROPERTIES OF CATALYTIC CURRENTS

Dependence of i_c on Concentration C^o

From equations (23) and (24) one concludes that the catalytic current is proportional to the concentration C^o of the substance which is regenerated by the catalytic process.

Dependence of i_c on Concentration C_Z^o and Rate Constant k_f

Since the catalytic current is a function of the product $k_f C_Z^o$ (see equation (23)), the influence of these two factors is discussed in the same section. Equations (23), (24) and (25) show that the catalytic current increases with $k_f C_Z^o$. However, there is no direct proportionality between i_c and $k_f C_Z^o$. For values of $k_f C_Z^o$ larger than 100 $sec.^{-1}$ the current is practically proportional to the square root of $k_f C_Z^o$ (see equation (27)). An example is described in the experimental part (Figure 5).

Dependence of i_c on the Head of Mercury

The dependence of the average catalytic current on the head of mercury is obtained by replacing m and t in equations (24) and (25) by their values in terms of the head of mercury H as corrected for the back pressure; t is inversely proportional to H^3. Since the equation showing the dependence

---

[3] See reference (25) page 67.

of i_c on H is rather intricate, it is easier to discuss a specific case. Average catalytic currents are plotted against H in Figure 4 for various values of $k_f C_Z^o$. The average total current obtained by adding the average diffusion current to (i_c) avg. is also plotted versus H in Figure 4. It is seen from Figure 4 that the catalytic current decreases when the head of mercury is increased. The larger the value of $k_f C_Z^o$, the less pronounced is the relative decrease in current. The total increases with the head of mercury, and the relative increase is more pronounced when $k_f C_Z^o$ decreases. For $k_f C_Z^o$ = 100 $sec.^{-1}$ it is found that the current is virtually independent of the head of mercury as one would expect from equation (27). (factor $m^{2/3}\ t^{2/3}$). When $k_f = 0$ the total current is simply the diffusion current which is proportional to $H^{1/2}$. The average catalytic current becomes inversely proportional to the head of mercury when $k_f C_Z^o$ approaches zero.

Influence of Temperature

The influence of temperature is obtained by differentiating (24) and (25) with regard to temperature. Various terms in the equation thus obtained can be combined as in the case of the Ilkovic equation[4]. Nevertheless, the writing is rather heavy and it is much easier to calculate k_f at various temperatures from the experimental current (see above). The energy of activation for the catalytic process is obtained from a conventional log k_f vs. 1/T plot.

---

[4] See reference (25) pages 74-76.

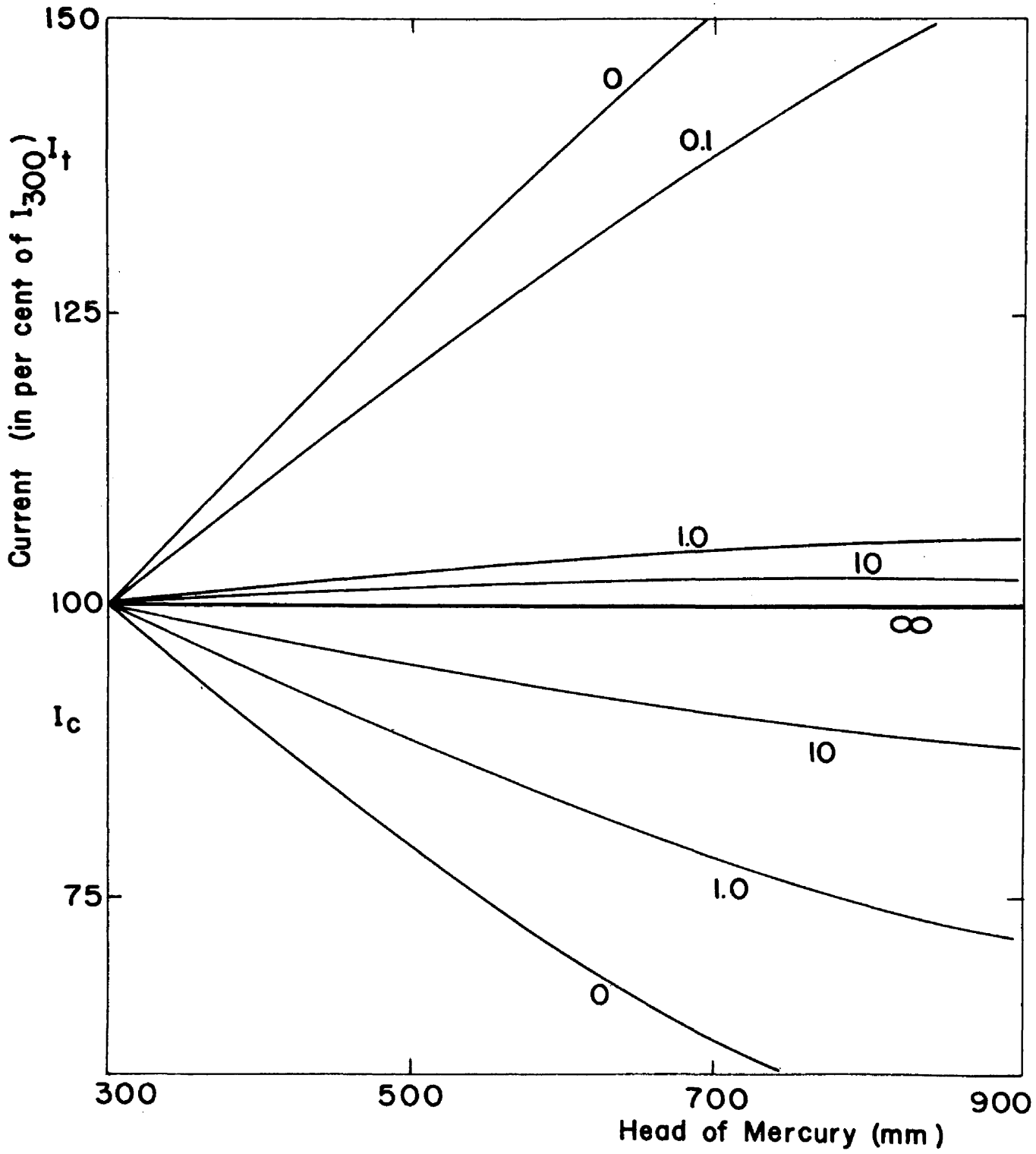

Figure 4. Variations of catalytic current with the head of mercury: $m = 1.5$ mg. sec.$^{-1}$ and $\tau = 4$ sec. for $H = 300$ mm. Number on each curve is the value of $k_f C_z^o$ in sec.$^{-1}$. Curves whose ordinates are higher than 100 represent the total current; curves whose ordinates are smaller than 100 represent the catalytic current.

CHAPTER III

EXPERIMENTAL STUDY

The theory developed in the previous chapter was applied to the catalytic wave obtained in the reduction of ferric ion in presence of hydrogen peroxide. This case of catalytic wave was thoroughly studied by Kolthoff and Parry (26), and only the results pertaining to the present theory will be discussed. In this case, the catalytic process is the oxidation of ferrous ion by hydrogen peroxide. This reaction involves two ferrous ions for each molecule of hydrogen peroxide, but the rate of the oxidation process is proportional to the product of the activities of ferrous ion and hydrogen peroxide (26). Consequently, the present theory is applicable without any change (see reaction (2)).

The experimental methods described by Kolthoff and Parry were followed without change. Waves were recorded with a Sargent Polarograph model XXI, and potentials were measured with a Leeds and Northrup student potentiometer. An H cell was used in all recordings; the calomel electrode arm of this cell was filled with a 1 molar potassium nitrate and an external calomel electrode was used. Unless otherwise indicated the temperature was $31.40 \pm 0.03^{\circ}$.

DESCRIPTION AND DISCUSSION OF EXPERIMENTAL RESULTS

Determination of Rate Constant k_f

Values of the catalytic current for concentrations of hydrogen peroxide[5] ranging from 0.0145 to 0.362 mole per liter are listed in Table 1 together with the corresponding rate constants determined from equation (27) and Figure 3. The supporting electrolyte was 0.25 molar H_2SO_4, and the following data were used in the calculations: $m = 1.52$ mg. $sec.^{-1}$, $t = 4.02$ sec., $C_{Fe^{+++}} = 2.5 \times 10^{-4}$ mole per liter. The diffusion coefficient of ferric ion was determined from the diffusion current for ferric ion in the absence of hydrogen peroxide, and the value $D_{Fe^{+++}} = 0.73 \times 10^{-5}$ $cm.^2$ $sec.^{-1}$ was obtained from the Ilkovic equation.

TABLE I

DATA FOR CATALYTIC CURRENTS OF FERRIC ION IN PRESENCE OF HYDROGEN PEROXIDE AT 31.4°

$C_{H_2O_2}$ mole per l.	Experimental (i_c) av microamp	Calcd. k_f $sec.^{-1}$ $(moles\ per\ l.)^{-1}$
0.0145	1.13	69
.0355	2.02	78
.0724	2.91	72
.181	5.18	72
.362	9.03	93
	Average	77

[5] Titrations of hydrogen peroxide were carried out by Mr. J. E. Strassner whose help is gladly acknowledged.

The rather large deviations from the average rate constant are caused mainly by experimental difficulties. Firstly, the waves are poorly defined (26); secondly, hydrogen peroxide undergoes catalytic decomposition during the measurements (26). Nevertheless, it can be concluded from the data of Table I that essentially the same value of k_f is obtained regardless of the hydrogen peroxide concentration.

Dependence of i_c on the Concentration of Hydrogen Peroxide

Variations of the catalytic current with the concentration of hydrogen peroxide are shown in Figure 5. The curves were calculated on the basis of the lowest and highest values of k listed in Table I, i.e., for $k_f = 69$ and $k_f = 93$ sec.$^{-1}$ (moles per liter)$^{-1}$, respectively. Points are experimental currents. Taking into account the relative inaccuracy of the experimental data, it can be concluded that the agreement between experimental and calculated data is good. The concentration of hydrogen peroxide was not lowered below 1.45×10^{-2} mole per liter since it was assumed in the previous theory that $C_{H_2O_2}$ is much larger than $C_{Fe^{+++}}$. In the present case $C_{Fe^{+++}}$ is 2.5×10^{-4} molar and the above condition would not have been fulfilled for values of $C_{H_2O_2}$ appreciably smaller than 1.45×10^{-2} mole per liter.

The relationship between catalytic current and concentration of ferric ion was not investigated, since the

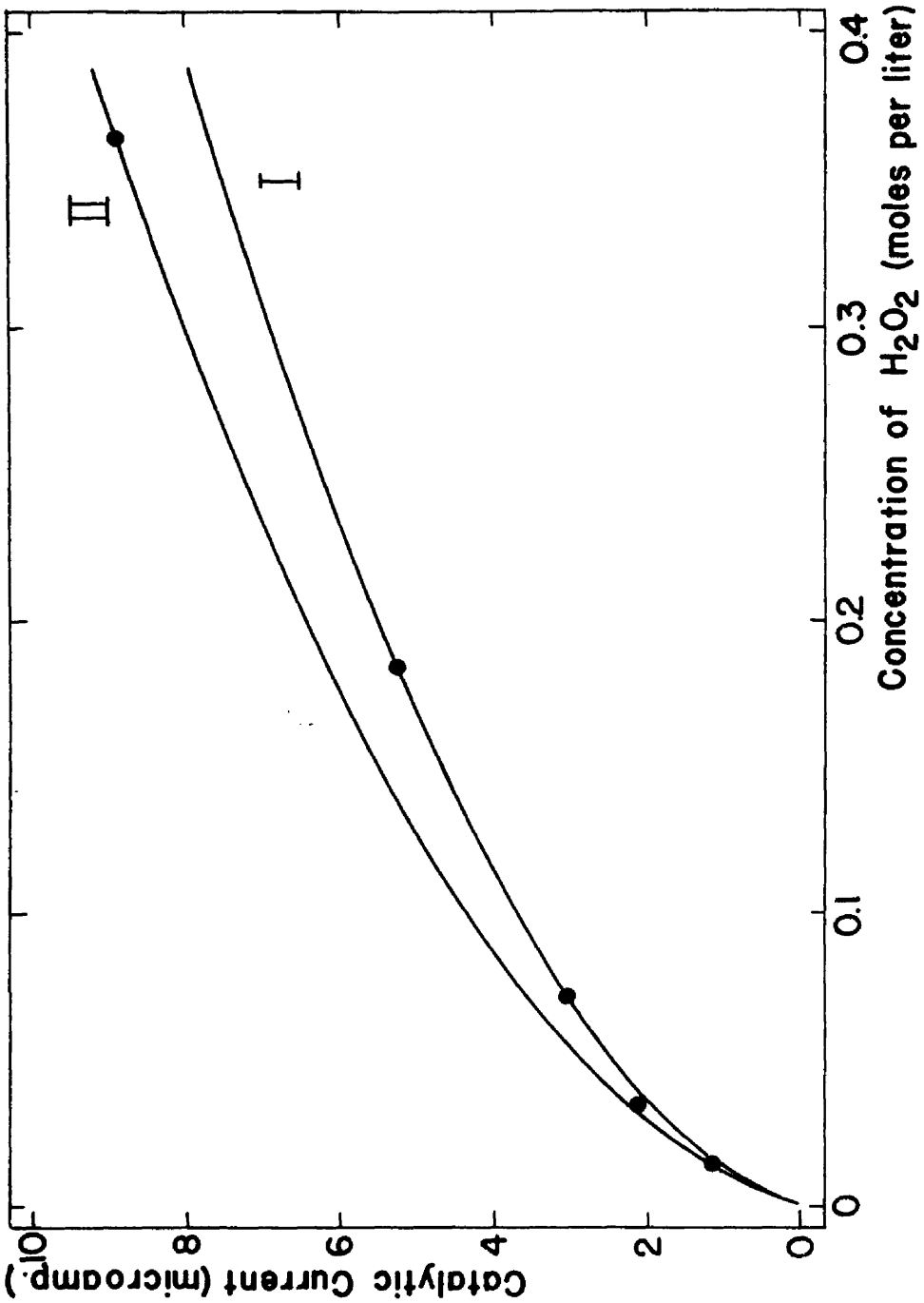

Figure 5. Variations of the catalytic current of ferric ion with the concentration of hydrogen peroxide. I, calculated curve for k_f = 69 sec.$^{-1}$ (moles per liter^{-1}); II, calculated curve for k_f = 93 sec.$^{-1}$ (moles per liter^{-1}). Dots are experimental values.

proportionality between these two quantities was verified by Kolthoff and Parry (26).

Dependence of i_c on the Head of Mercury

Data for three values of the head of mercury are listed in Table II.

TABLE II

VARIATIONS OF i_c WITH THE HEAD OF MERCURY

H,[6] mm.	Experimental (i_c) av. microamp	Calcd. (i_c) av. microamp
611	2.02	2.01
727	1.96	1.95
886	1.65	1.74

The following data were used in the calculations: $C_{H_2O_2} = 3.55 \times 10^{-2}$ mole per liter, $C_{Fe^{+++}} = 2.5 \times 10^{-4}$ mole per liter, $D_{Fe^{+++}} = 0.73$ cm.^{2} sec.$^{-1}$, r: 4.02, 3.40 and 2.71 sec., respectively; m, 1.52, 1.82 and 2.25 mg. sec.$^{-2}$, respectively. The average value $k_f = 77$ sec.$^{-1}$ (mole per liter)$^{-1}$ of Table I was used in calculations. Table II shows that the agreement between experimental and calculated data is good. The total current remained practically unchanged in agreement with previous observations of Kolthoff and Parry (26).

---

[6] Not corrected for back pressure

Dependence of $(i_c)_{av}$ on Temperature

The catalytic current was measured at 0.6° and rate constant k_f was calculated on the basis of the following data: $C_{Fe^{+++}} = 2.5 \times 10^{-4}$ mole per l., $D_{Fe^{+++}} = 0.25 \times 10^{-5}$ cm.^{2}sec.$^{-1}$, r = 4.23 sec.; $C_{H_2O_2}$: 0.0344, 0.0687 and 0.172 mole per l., respectively; i_c: 0.317, 0.581 and 1.195 microamp., respectively. The corresponding values of k_f were as follows: 14, 18, and 29 sec.$^{-1}$ (moles per l)$^{-1}$. Logarithms of extreme values of k_f obtained at 31.4 and 0.6° are plotted against the reciprocal of absolute temperature in Figure 6, which shows that the polarographic values of k_f are in good agreement with the data obtained by a chemical method by Baxendale, et al. (2).

The polarographic values of k_f at 0.6° are slightly too high as indicated by Figure 6. This can be explained as follows. The polarographic cell was immersed in the water-bath at 0.6°, but the tube connecting the capillary of the dropping mercury electrode to the mercury reservoir was not. As a result, the mercury dropping in the cell, and the solution surrounding the mercury drop, were at a temperature above 0.6°. Therefore, the rate constants thus obtained are too high. A completely immersed cell was not used because the manipulations of such a cell would have prolonged the operations involved in the recording of a wave to a point where the catalytic decomposition of hydrogen peroxide would have interfered.

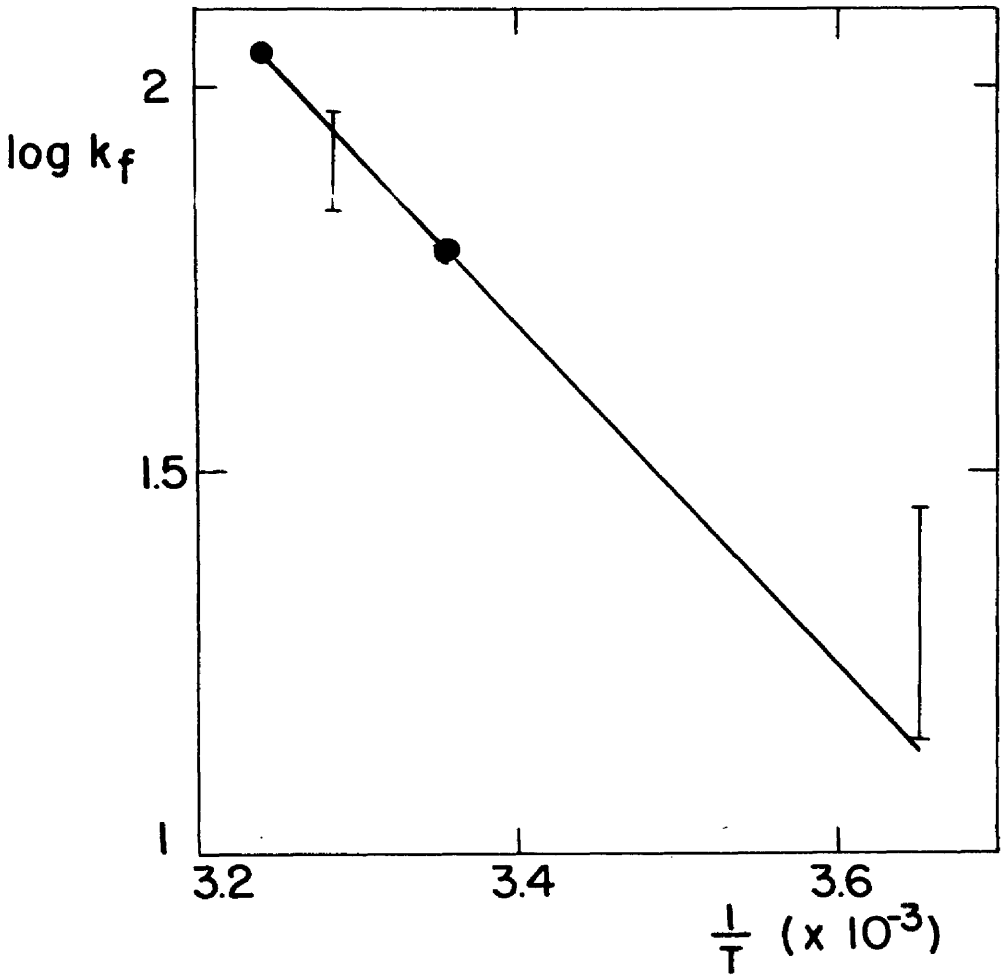

Figure 6. log k_f vs. (1/T) plot for the oxidation of ferrous ion by hydrogen peroxide. Dots are values obtained by a chemical method by Baxendale, et al. Vertical lines represent extreme polarographic values.

CONCLUSION

The theory developed in the present dissertation accounts quantitatively for the properties of catalytic waves. Since rate constants can be determined from polarographic data,[7] catalytic currents can be used in the study of kinetic processes which are too rapid to be followed by conventional methods. Likewise, reactions involving unstable substances can also be studied. However, it should be pointed out that the occurrence of a catalytic wave requires the fulfillment of certain conditions which limit somewhat the scope of the method.

NOTE:

Part I of this dissertation was published in the Journal of the American Chemical Society, 74, 3500-3506 (1952).

---

[7] The fluctuations observed for the catalytic current of ferric ion in presence of hydrogen peroxide result mainly from experimental difficulties rather than from approximations in the theoretical treatment.

PART II

INFLUENCE OF POTENTIAL AND pH ON THE KINETICS OF THE ELECTROLYTIC OXIDATION OF METALS

CHAPTER IV

INTRODUCTION

The study of the electrolytic oxidation of metals is of great significance with regard to the interpretation of metallic corrosion in aqueous solutions. Many investigations of the anodic oxidations of metals have been made, but all too often the variables which might affect the oxidation rate have not been carefully controlled. For example, polarization curves for the oxidation of metals have often been obtained either in unbuffered solutions or in buffered solutions containing undesirable constituents. When unbuffered solutions are used, the results are often invalidated because of variations in the hydrogen ion activity in the course of the electrolysis. When buffered solutions are used, certain constituents of the buffer system generally interfere because of the formation of a complex ion or a precipitate with the cation of the metal being studied. In other investigations on the kinetics of the oxidation of metals, the potential of the metal undergoing dissolution is not controlled. This result in variations of potential during the oxidation process, and the interpretation of the results, is greatly complicated. It is not intended by the above comments to detract from the many excellent investigations of the electrolytic oxidation of metals, but rather to emphasize the need for

a rational approach in this field. Such an approach is believed to have been followed in the present dissertation.

CHAPTER V

THEORETICAL PRINCIPLES

EQUILIBRIUM CONDITIONS

The first logical step in a kinetic study is to determine the conditions characterizing the equilibrium the system being studied may possibly reach. Such equilibrium conditions are determined from general thermodynamic principles. In electrochemical systems involving aqueous solutions the two most important variables are the potential of the electrode being studied and the hydrogen ion activity of the aqueous solution. These two variables can be correlated to the activity of the soluble species involved in the electrode process on the basis of the Nernst equation. From a practical standpoint it is convenient to replace the terms containing the logarithm of the hydrogen ion activity by their corresponding pH values in the resulting equations. This substitution involves a minor approximation which causes a slight error that can generally be disregarded in the present type of study. The resulting formula can be written as an equation expressing the potential of the electrode being studied as a function of several variables, among which is the pH of the electrolyte. If all the variables, except the pH, are kept constant the electrode potential is solely a function of pH, and the variations of these functions can be represented graphically.

Such a representation is made in the form of a potential-pH diagram. Diagrams of this type were first used by Clark (9) in the interpretation of the electrochemical equilibria: hydrogen ion - hydrogen, and oxygen - water. Potential - pH diagrams were also used by Michaelis (34) in the study of organic redox systems. Pourbaix has extended the use of potential-pH diagrams to the interpretation of the electrochemical behavior of metals and also to metallic corrosion (14, 15, 16, 40). In addition, potential-pH diagrams have a great didactic value (7, 13).

Despite their usefulness, potential-pH diagrams have the very serious limitation of presenting only equilibrium conditions. Kinetic considerations are not taken into account in the preparation of these diagrams, and the information supplied by them can be misleading. For example, the range of potentials in which a metal actually undergoes anodic dissolution can be very different from the potentials at which one would expect this reaction to occur on purely thermodynamic grounds. Nevertheless, potential-pH diagrams are very useful as a guide in the experimental study of electrochemical equilibria.

From the above considerations one infers that it is desirable to control the two variables, potential and pH, which are preponderant in determining the conditions for electrochemical equilibrium. This was done in the present investigation. Such an approach was made possible by the recent development of potentiostats, i.e. instruments for

electrolysis with automatic control of the potential of one electrode. The first instrument of this type was described by Hickling (22) who coined the term "potentiostat." Since then, potentiostats involving various instrumental principles have been developed, and many interesting applications have been made in the field of electro analysis (30). The method has also been applied to the study of a few electrochemical problems (10, 28, 41, 42). The pH of the electrolyte in which the metal is oxidized can of course be controlled by a buffer, but such a method has its drawbacks as pointed out in Chapter IV. A different method in which either acid or base is added automatically in order to keep the pH constant was developed in the course of this study.

APPROXIMATE TREATMENT OF THE KINETICS OF THE ANODIC OXIDATION OF METALS AT CONTROLLED POTENTIAL

Case in which the Reaction Products are Soluble

The anodic oxidation of metals is a heterogeneous process, and it is therefore of interest to determine the effect of the mass transfer process on the kinetics of the over-all process. This will be done here in an approximate manner, mainly in order to determine the various variables, besides potential and pH, which have to be controlled.

Consider the electrolytic dissolution of a metal M at constant potential, and let the ion M^{+n} be the reaction product. The rate of dissolution per unit area is

$$\frac{dN}{dt} = k_a - k_c C_{x=o} \tag{28}$$

where dN/dt is the number of moles of ion M^{+n} produced per unit of time, $C_{x=o}$ is the concentration of ion M^{+n} at the surface of the metal M, at a given time of electrolysis, and k_a and k_c are the rate constants for the anodic and cathodic processes, respectively. Note that k_a and k_c are rate constants for an heterogeneous process, and are expressed in moles $cm.^{-2}$ $sec.^{-1}$ and $cm.\ sec.^{-1}$ respectively. These rate constants depend on the electrode potential as was shown in many experimental studies and in a development of the absolute rate theory (19).

The current at a given time after the beginning of the electrolysis is directly obtained from equation (28) by multiplying the rate dN/dt by the area of the electrode and by the charge involved in the production of one mole of ion M^{+n}. Thus

$$i_t = nFA(k_a - k_c C_{x=o}) \tag{29}$$

where n is the number of electrons involved in the electrode process, F the Faraday, and A the area of the electrode. In subsequent treatment it will be assumed that the area of the electrode remains constant during the dissolution process, i.e. it is assumed that there is no preferential attack in some part of the electrode.

The current i_t can also be expressed in terms of the gradient of concentration of ion M^{+n} at the electrode surface.

If a large excess of an indifferent electrolyte is present in solution it is permissible to neglect electric migration, and the current is

$$i_t = -nFAD\left(\frac{\partial C}{\partial x}\right)_{x=0} \qquad (30)$$

where D is the diffusion coefficient of ion M^{+n}.

The exact calculation of $(\partial C/\partial x)_{x=0}$ is exceedingly difficult in the case of a stirred solution (3, 29), and it is much easier to use a less rigorous approach and to express the gradient of concentration $(\partial C/\partial x)_{x=0}$ in terms of the thickness of the diffusion layer (36, 37). Thus

$$\left(\frac{\partial C}{\partial x}\right)_{x=0} = -\frac{C_{x=0} - C_t}{\delta} \qquad (31)$$

where C_t is the bulk concentration of ion M^{+n} at time t. The concentration C_t can be expressed in terms of the current i_t by applying Faraday's law. Hence

$$C_t = \frac{\int_0^t i\,dt}{nFV} \qquad (32)$$

where V is the volume of the solution in which the electrolytic oxidation is carried out. By combining equations (29), (30), (31), and (32), one obtains a differential equation whose solution is

$$i_t = nFAk_2 \exp\left[-\frac{AD}{V\delta\left(\frac{D}{k_c\delta}+1\right)}t\right] \qquad (33)$$

The integration constant n F A k_a in equation (33) was determined by recalling that at time t=o, $C_{x=o} = 0$, and i_o = n F A k_a according to equation (29).

The loss of weight of the electrode after a given electrolysis time can be calculated from equation (33) if one assumes that the thickness of the diffusion layer δ is independent of time. By the application of Faraday's law and a few simple transformations one obtains from equation (33) the following value for the loss of weight:

$$W = W_A k_a \left\{ \frac{1}{\lambda \tau} \left[1 - \exp(-\lambda \tau) \right] \right\} \qquad (34)$$

where λ is defined by the following relationship

$$\lambda = \frac{AD}{V\delta\left(\frac{D}{k_c \delta} + 1\right)} \qquad (35)$$

in which W is expressed in the units g. cm.$^{-2}$ sec.$^{-1}$, W_A is the atomic weight of the metal M, and τ is the duration of electrolysis in seconds.

Several important conclusions can be drawn from equations (33) and (34).

(1) The current decreases exponentially with time; hence, a plot of the logarithm of the current i_t <u>versus</u> time should yield a straight line.

(2) The current at a given time t is virtually an exponential function of the electrode potential. This results from the exponential dependence of the rate constant k_a on potential. Actually, the above conclusion is correct only when the

influence of the cathodic process can be neglected, i.e. when the potential is sufficiently anodic, for example, 0.1 volt more anodic than the equilibrium potential.

(3) The loss of weight W for a given electrolysis time τ is an exponential function of the potential, since W is proportional to k_a. This conclusion is also valid only when the potential is appreciably more anodic than the equilibrium potential. When the influence of the cathodic process becomes noticeable, the loss of weight is smaller than the value of W one would expect if the cathodic process were negligible.

(4) The loss of weight W varies in the course of time. In order to elaborate on this point it is convenient to plot the value of $W/W_A k_a$ from equation (34) versus the dimensionless group $\lambda\tau$ (Fig. 7). Noting that $W/W_A k_a$ is proportional to the loss of weight W at a given potential, it is seen from Fig. 7 that there is a marked variation of the loss of weight per unit area and per unit of time in the course of the electrolysis. At time $\tau = 0$ one calculates the limiting value of $W/W_A k_a = \infty$. Notice that a plot of the logarithm of the quantity $W/W_A k_a$ versus $\lambda\tau$ is not too different from a straight line for limited variations of $\lambda\tau$.

(5) The loss of weight is a function of the volume of the solution in which the electrolysis is carried out. Equations (33) and (34) show that at a given time of electrolysis, the loss of weight and the current i_t should increase as the volume of solution is increased.

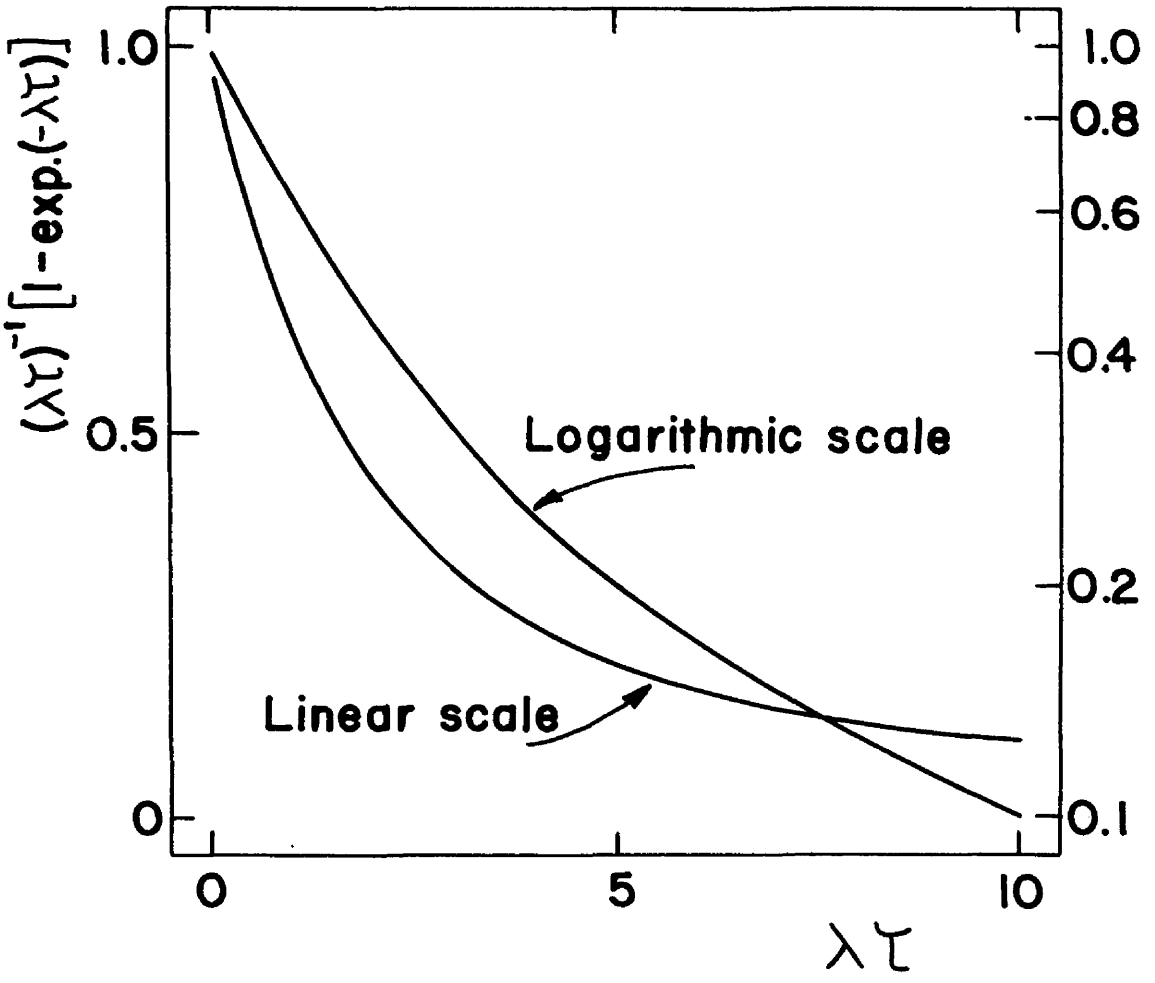

Figure 7. Variations of the ratio W/W_A k_a with the quantity $\lambda\tau$ (see equation (34)).

(6) The current i_t and the loss of weight W are dependent upon the efficiency of the stirring of the solution. The thickness of the diffusion layer δ decreases when the stirring becomes more efficient, and consequently λ increases. From Fig. 7 it is seen that the time τ required to reach a given value of W decreases as λ increases. Hence, the rate of oxidation increases when the stirring becomes more efficient. The same conclusion can be drawn from equation (33).

(7) The thickness of the diffusion layer δ depends on the geometric dispositions of the electrolytic cell, and therefore the position of the electrode in the electrolytic cell must remain unchanged in comparative tests.

It should be emphasized that the conclusions drawn from equations (33) and (34) are of an approximate character since it was assumed in the derivation of these equations that the thickness of the diffusion layer δ is independent of time. Actually δ depends on the concentration of ion M^{+n}, i.e. on the electrolysis time, but one can assume, as a first approximation, that δ is constant.

In noting the large number of variables which can influence the rate of anodic oxidation of a metal it becomes apparent that absolute rates of dissolution are somewhat meaningless. Only by the use of comparable data obtained under similar conditions can any valid interpretation be made.

Kinetics of Anodic Oxidation in Cases Involving the Formation of an Insoluble Product.

When an insoluble species is formed in the course of the oxidation of a metal, the effective area of the metal generally varies in the course of the electrolysis because of the partial coating of the electrode. Furthermore, the coating of the electrode may result in a marked increase in the electrical resistance at the metal-solution interface. Such phenomena can be taken into account by introducing more or less arbitrary parameters in the derivation of an equation for the current during oxidation. However, an equation derived in such a manner would probably lead to uncertain conclusions, but two remarks of a qualitative nature can be made: (1) Because of the coating of the electrode, currents are generally smaller than one would expect if there were no coating; (2) the increase in the loss of weight as the potential becomes more anodic, is smaller than the increase one would expect if there were no coating, all other experimental conditions being the same. Thus, if W_t is plotted against potential, the resulting curve levels off progressively as the potential becomes more anodic.

CHAPTER VI

EXPERIMENTAL METHODS

GENERAL PROCEDURE

The electrode properly prepared as described below was oxidized at controlled potential for two hours, the pH of the electrolyte being automatically kept at a constant value. The loss of weight of the electrode was determined after electrolysis and rate of oxidation was computed from this datum and from the area of the electrode, it being assumed that the roughness factor is equal to unity.

EXPERIMENTAL APPARATUS

The major components of the apparatus used in this investigation were: the electrolytic cell, the potentiostat, and the unit for automatic control of pH. These elements of the apparatus will now be described. The general arrangement of the apparatus is shown in Fig. 8.

The Electrolytic Cell (Figure 9)

The electrolytic cell was a 1 liter beaker immersed in a constant temperature water jacket. Three electrodes were immersed in the cell: the metallic specimen S, the auxiliary electrode A, and the reference electrode R. The construction and mounting of the specimen is described below. The auxiliary electrode A was composed of a platinum electrode immersed in a glass sleeve closed at the bottom by a coarse fritted glass

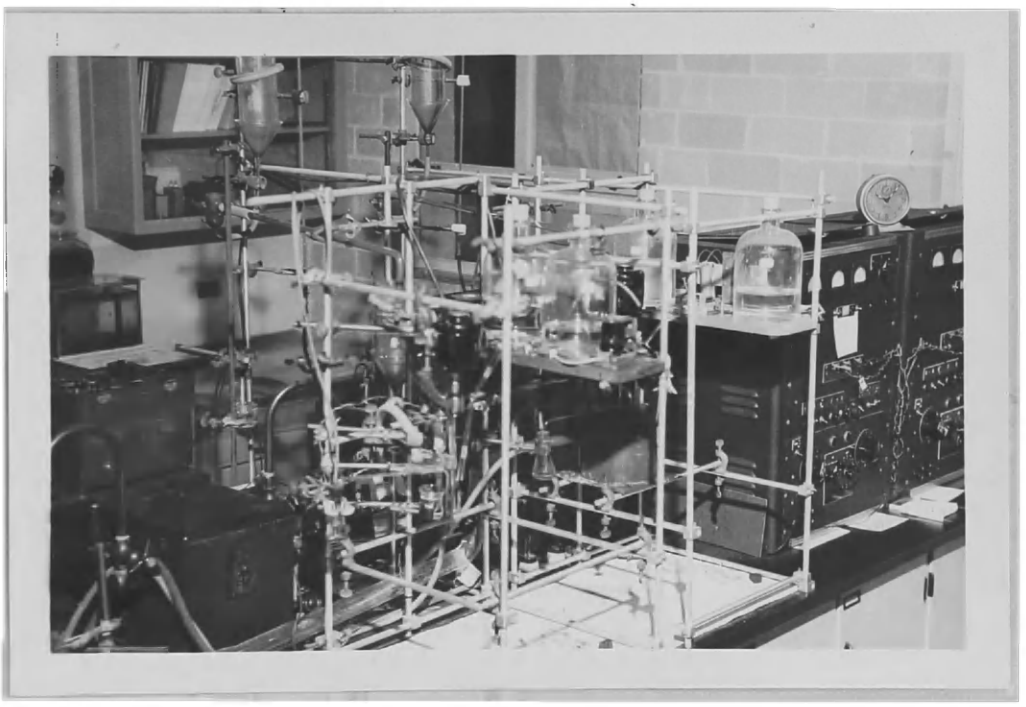

Figure 8. General arrangement of the apparatus.

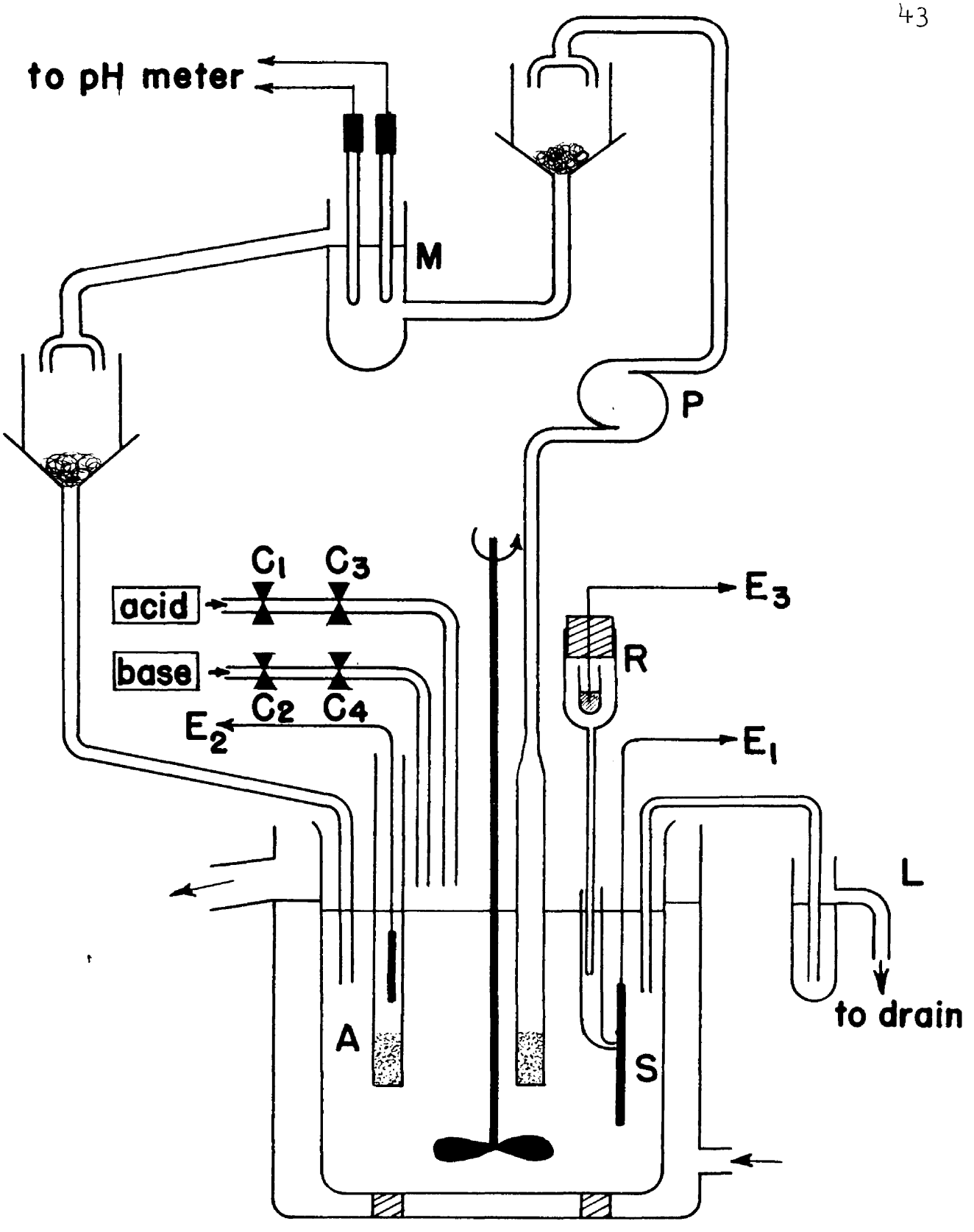

Figure 9. Electrolytic cell and auxiliary equipment.

disk. The solution in the glass sleeve was the same as that in the electrolytic cell. The reference electrode included an agar-agar salt bridge to prevent the diffusion of chloride ion into the cell. The tip of the glass tube covering the reference electrode was pressed against the specimen S in order to avoid errors resulting from the ohmic drop in the solution (21). The electrodes S, A, and R were connected to the potentiostat which is described below. The solution was stirred at a constant speed, and the level of the liquid in the beaker was kept constant by means of the device L.

The pH of the solution was kept constant during electrolysis by the addition of acid or base. This addition of reagent was accomplished by a gravity flow system which was controlled by magnetic clamps C_1 and C_2. These clamps were operated by an automatic unit which is described below. The operation of this automatic unit was regulated by the signal from a glass-calomel electrode couple immersed in cell M. A conventional glass electrode (Beckman #1190-90) was used up to pH 11.5 and suitable corrections were made in the alkaline range. A few tests were made with the special lithium glass electrode (Beckman, blue tip, #1190-E), but the response of this electrode was too slow to control the addition of reagent satisfactorily. At and above pH 13 no automatic control was needed. The solution in the cell M was continuously renewed by means of the circulating pump, P, and the solution was dropped in the funnels F from a height of approximately 15 cm. Splashing was avoided by a cylinder

lf large diameter glass tubing. The purpose of this circulating system was to insulate electrically the cell M from the main electrolytic cell. It was observed that, when this precaution was not taken, the behavior of the pH control unit was very erratic due to leaks to ground. It should be pointed out that connection E_1 is grounded, and that the pH control unit is fed by the 110 volt (A.C.) mains. As a result, leaks in the circuit of the pH unit are sufficient to interfere with the operating of the first stage of amplification of the pH measuring device.

In order to shorten the delay in the response of the pH control unit the volume of solution in cell M was reduced to a minimum (10 ml). Likewise, rather narrow (4 mm. internal diameter) tubes were used in the circulating system.

Potentiostat (Figure 10)

The potentiostat used in this investigation is a modification of the instrument described by Lamphere and Rogers (27). The instrument described by these authors was designed for electroanalysis, and several modifications had to be introduced to adapt the instrument to the present investigation. The control element of the potentiostat, however, was the same as the instrument of Lamphere and Rogers. The electrolysis current was supplied by two transformer-rectifier units. T_1 and T_2 were isolation transformers, and T_3 and T_4 were adjustable autotransformers. The output of transformers T_3 and T_4 was rectified and

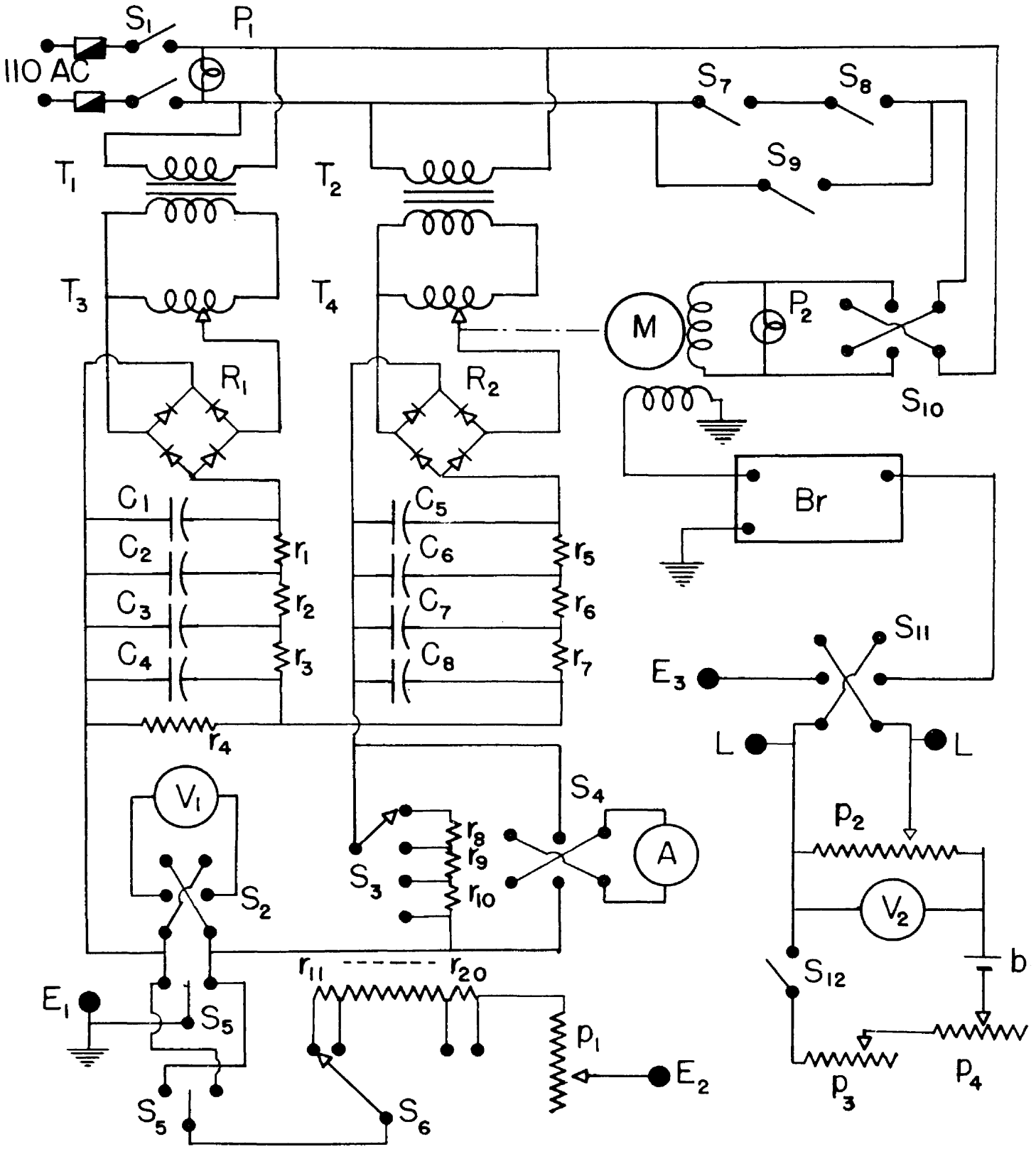

Figure 10. Schematic diagram of the unit for electrolysis at controlled potential.

filtered. One of the autotransformers was driven by a Brown reversible motor M; the other autotransformer was operated manually. The maximum output voltage of the latter transformer was mechanically limited to 30 volts, whereas the maximum output of the former transformer was 135 volts. These output voltages were in opposition so that the polarity of the voltage applied to the electrolysis cell could be reversed. The electrolytic cell was connected at E_1 (the specimen electrode) and E_2 (the platinum auxiliary electrode), and the current through the cell was measured with an ammeter, A, having sensitivities of 0.005, 0.05, 0.5, and 5 amperes, respectively. The voltage applied to the cell was read on the 0-250 volt voltmeter, V. The meters A and V were equipped with reversing switches.

An adjustable resistance (S_6 and P_1) was connected in series with the electrolytic cell in order to use the autotransformer, T_4 (which is driven by motor M) in the upper part of its range. This was advantageous because in this region the voltage increment per winding tapped by the brush is small in comparison with the total output voltage, and hence a somewhat more sensitive control was achieved.

The difference of potential between the specimen (E_1), which was always grounded, and the reference electrode (E_3) was compensated by the voltage supplied by potentiometer p_2. This compensating voltage was approximately read on the "Helipot" potentiometer p_2, and was accurately measured by means of a student potentiometer (Leeds and Northrup #7651)

connected to terminals LL. The transformer T_4, driven by motor M, responded to any difference of potential larger than 0.002 volt, between the electrode couple E_1 - E_3 and the output of the potentiometer p_2. The limit switches S_7 and S_8 disconnected one winding of the motor M as the autotransformer T_4 neared the ends of its range.

The elements of the circuit as shown in Figure 10 were as follows: T_1, isolation transformer, 350 watts; T_2, isolation transformer, 150 watts; T_3 and T_4, "Powerstat" transformer, 3 amp output; R_1, selenium bridge rectifier, 144 volts, p.9 amp.; R_2, selenium bridge rectifier, 168 volts, 2.4 amp.; C_1 to C_4, electrolytic condenser, 125 microfarads, 350 volts; C_5 to C_8, electrolytic condenser, 250 microfarads, 350 volts; r_1 to r_3, 25 ohms, 50 watts; r_4, 40 ohms, 200 watts; r_5 to r_7, 10 ohms, 200 watts; r_8 to r_{10}, shunts for meter A to give readings of 0.05, 0.5, and 5 amp., respectively; r_{11}, 20 K., 20 watts; r_{12}, 10 K., 20 watts; r_{13}, 5 K., 20 watts; r_{14}, 2 K., 20 watts; r_{15}, 1 K., 20 watts; r_{16}, 500 ohms, 50 watts; r_{17}, 200 ohms, 100 watts; r_{18}, 100 ohms, 100 watts; r_{19}, 50 ohms, 100 watts; r_{20}, 25 ohms, 200 watts; p_1, potentiometer, 16 ohms, 100 watts; p_2, "Helipot" potentiometer, 1000 ohms, 10 turns, 0.1%; p_3, potentiometer, 2000 ohms, wire-wound; p_4, potentiometer, 200 ohms, wire-wound; S_5, D.P.D.T. switch; S_7 and S_8 limit switches; S_9 push-button switch; b_1, 6 volt storage battery; Br, "Brown" amplifier, model #356358-1; M, "Brown" reversible motor, model #76750-3; V_1, 0-150 volt, voltmeter; V_2, 0-3 volt, voltmeter; A, 0-5 milliamp. ammeter.

Unit for Automatic Control of pH

The addition of acid or base to the solution in the electrolytic cell was controlled by the unit shown in Figure 11. A Beckman, model G, pH meter was used as the measuring device. Resistance r_1 (terminals MM) was connected in the second amplifier stage of this instrument and the ohmic drop in resistance r_1 was balanced against the voltage on the terminals of resistance r_2. When there was a difference between the prescribed and the actual pH of the solution in the electrolytic cell, relay R was actuated and either thyraton T_1 or T_2 became conductive. As a result, magnetic clamp C_1 or C_2 (see Figure 9) controlling the addition of base or acid to the electrolytic cell was open until the pH of the solution in the electrolytic cell had reached the prescribed value. At that moment the addition of base or acid was stopped automatically. The precision of the control was ±0.1 pH unit, except in the pH range 6 - 8 where the precision was ±0.3 pH unit.

The elements of the circuit shown in Figure 11 were as follows: r_1, 1500 ohms, 2 watts; r_2, 100 ohms, 2 watts; r_3, 400 ohms, 200 watts, adjustable; r_4 and r_5, 100 K, 2 watts; r_6 and r_7, 30 ohms, 2 watts; r_8 and r_9, 1 K, 2 watts; r_{10} and r_{11}, 100 K, 2 watts; p_1, potentiometer, 400 ohms, wire-wound; p_2, potentiometer, 20 ohms, wire-wound; C_1, electrolytic condenser, 250 microfarads, 350 volts; C_2 and C_3, A. C. condenser, 10 microfarads; b_1, 1.5 volt dry cell; b_2, 45 volt dry cell; T_1 and T_2, thyratron, 2050; MM terminals

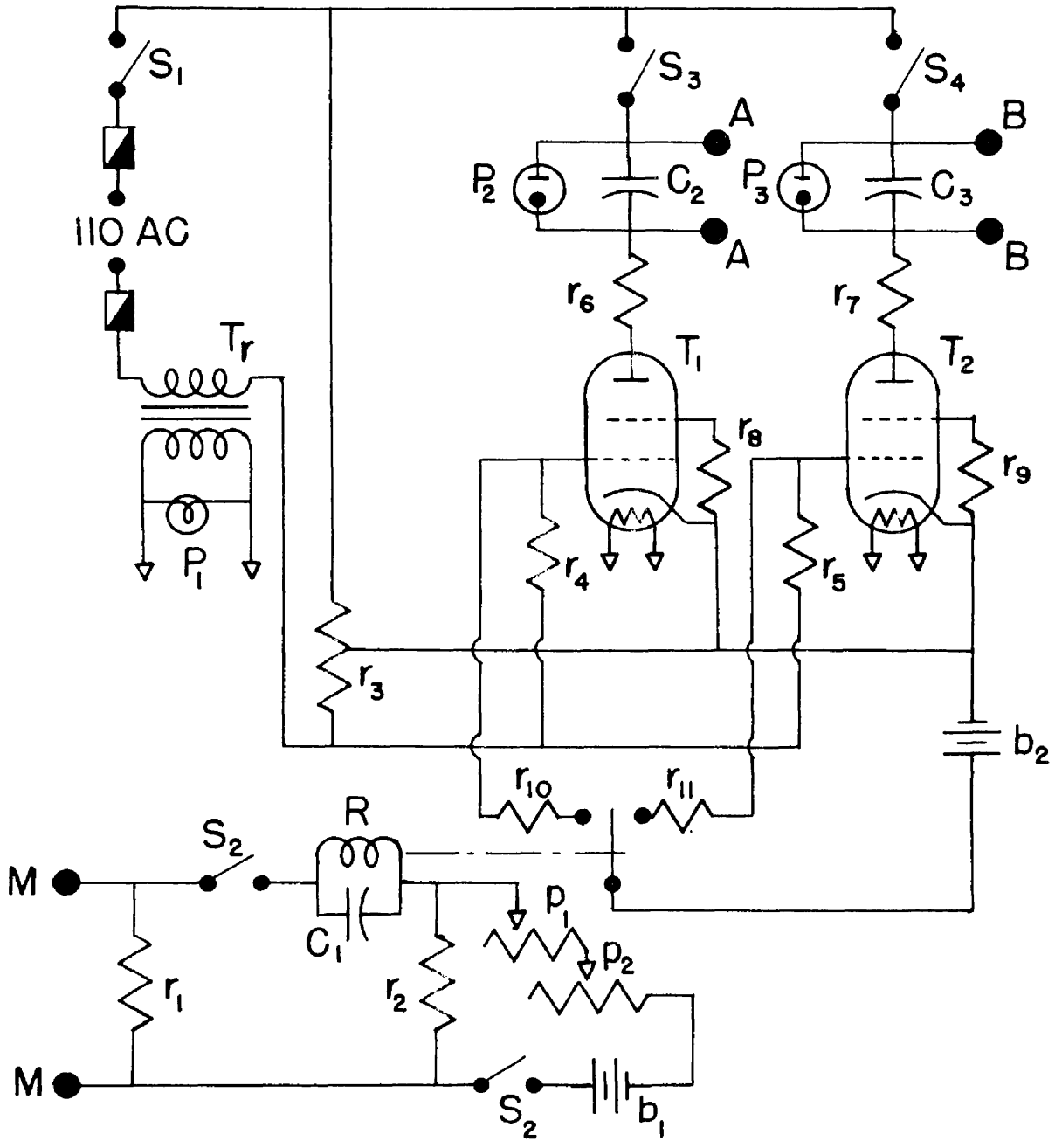

Figure 11. Schematic diagram of the unit for pH control during electrolysis.

connected to the Beckman pH meter (see above); AA and BB terminals connected to the coils of magnetic clamps C_1 and C_2 (see Figure 9).

SOLUTIONS AND PREPARATION OF SPECIMENS

Experimental conditions pertaining to the composition of the electrolyte, preparation of specimens, etc., are listed in Table III.

TABLE III

EXPERIMENTAL CONDITIONS OF ELECTROLYSIS

Metal	Electrolyte	Cleaning Solution and Duration of Immersion	
Iron	0.1 M SO_4^{--}	6 M HCl	15 - 30 seconds
Tin	0.1 M SO_4^{--}	6 M HCl	15 - 30 seconds
Lead	0.1 M ClO_4^{-}	6 M $HClO_4$	15 - 30 seconds

The acid solution used in the pH control unit was of the appropriate acid of the anion selected. Its concentration varied from 0.1 to 0.001 M depending upon the pH range of the solution in the cell. A proper quantity of the sodium salt of the anion was added to the acid solution to maintain the concentration of the selected anion at 0.1 M. Likewise, the solution of sodium hydroxide used in the pH control unit was maintained at a concentration of 0.1 M in the anion selected, and its concentration in sodium hydroxide varied from 0.1 to 0.001 M according to the desired pH chemicals.

All electrolysis were carried out at 35± 0.1° C., and the duration of electrolysis was two hours in all experiments.

"Pure" metal[8] specimens were cleaned with acetone and a copper wire was soldered to one edge of each specimen. The specimens were then coated with a polystyrene preparation[9], except for a 1 cm x 1 cm test area and the far end of the lead. This clear area was near the center of the specimen in order to minimize abnormal rates of oxidation induced by cutting and soldering the specimen. The samples were dried in air for about twenty minutes and then placed in an oven (80° C.), where they could be kept for long periods without noticeable corrosion of the open test area. The minimum stay in the oven was about twelve hours to insure the evaporation of the toluene solvent from the polystyrene coating before the specimen was weighed.

Just before use, the coated specimen was weighed on an analytical balance, and the dimensions of the test area were taken. Immediately before the electrolysis, the specimen was dipped into the cleaning solution (see Table III) for 15 - 30 seconds in order to remove any film of oxide, etc., which might have been formed during the drying. The specimen was then rinsed with distilled water. The immersion in the cleaning solution was not prolonged enough

---

[8] Obtained from D. H. Mackay, 198 Broadway, New York, N. Y.

[9] This preparation is commonly known as "Q-Dope" or Polystyrene cement and coil dope.

to lead to measurable loss of weight. The electrolysis was started immediately after the cleaning operation.

At the end of the electrolysis, the samples were rapidly removed from the electrolysis cell, cleaned by dipping them into the cleaning solution (see Table III)-- again not long enough to effect measurable loss of weight--rinsed with distilled water, dried with filter paper, and placed under vacuum in a desicator. The samples were dried for at least two hours prior to final weighing. Weight losses of 0.5 - 1.0 milligrams were detectable by this procedure.

CHAPTER VII

DESCRIPTION AND DISCUSSION OF RESULTS

I - THE ELECTROLYTIC OXIDATION OF IRON

Variations of the Loss of Weight with the Duration of Electrolysis

Losses of weight are plotted against the time of electrolysis in Figure 11 for the dissolution of iron in 0.1 M sulfuric acid at a potential of -0.290 volts vs. the normal hydrogen electrode[10]. The value of λ corresponding to the present experimental conditions was calculated from equation (34) for the data corresponding to $\tau = 4$ hours, and the resulting theoretical curve is also shown in Figure 12. The agreement between experimental and calculated results is as good as one could expect from the approximate treatment of Chapter V. The important conclusion to be drawn from the diagram of Figure 12 is that the rate of oxidation should be measured for a constant duration of electrolysis. This conclusion which was drawn from the treatment of Chapter V is thus confirmed experimentally.

Influence of the Anion on the Rate of Oxidation of Iron

The nature of the anion in an electrolyte in which a metal undergoes anodic oxidation greatly influences the rate of oxidation. This influence of the anion is not yet

---

[10] The European convention of the sign of potential will be used throughout this work.

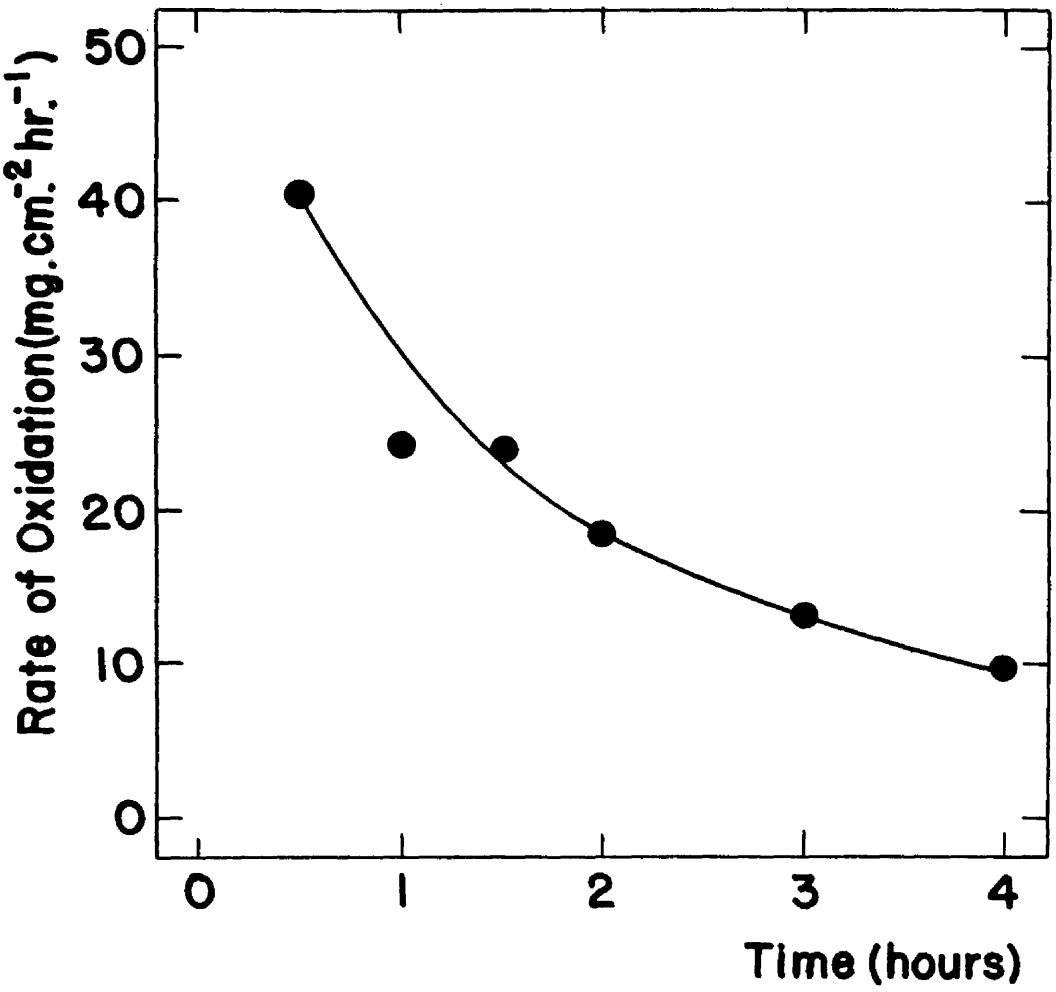

Figure 12. Variation of the rate of oxidation of iron with duration of electrolysis. (see text for experimental conditions)

fully understood, although several systematic studies have appeared in the recent literature (39). This effect of the anion on the rate of oxidation of iron is shown in Figure 13 in which rates of oxidation are plotted against potential for various anions at a concentration of 0.1 M. Samples were oxidized for two hours in tenth-molar solutions of the following acids: Perchloric, hydrochloric, sulfuric, acetic, and phosphoric acids. It is seen from this diagram that, at a given potential, the rate of dissolution is the lowest for perchloric acid and the highest for phosphoric acid. Notice that there is almost a hundredfold increase in rates of dissolution from perchloric to phosphoric acid. This shows how important it is to have the same anion in the electrolyte being used in electrolysis at varied pH. In the present work in which experiments are carried out over the whole range of pH's, electrolytes containing acetate or phosphate ions had to be disregarded because of the formation of insoluble salts in the neutral or alkaline range. Chloride was disregarded because of the possibility of chlorine production at highly anodic potentials, and also because of the formation of chloro-complexes. Between perchlorate and sulfate ions, the latter ion was selected for the study of iron, because of the danger of electrolytic reduction of perchlorate in the presence of redox couples involving iron.

Influence of Potential and pH on the Rate of Oxidation of Iron

Variations of the rate of oxidation with potential are shown in Figure 14 for various pH's, and additional results

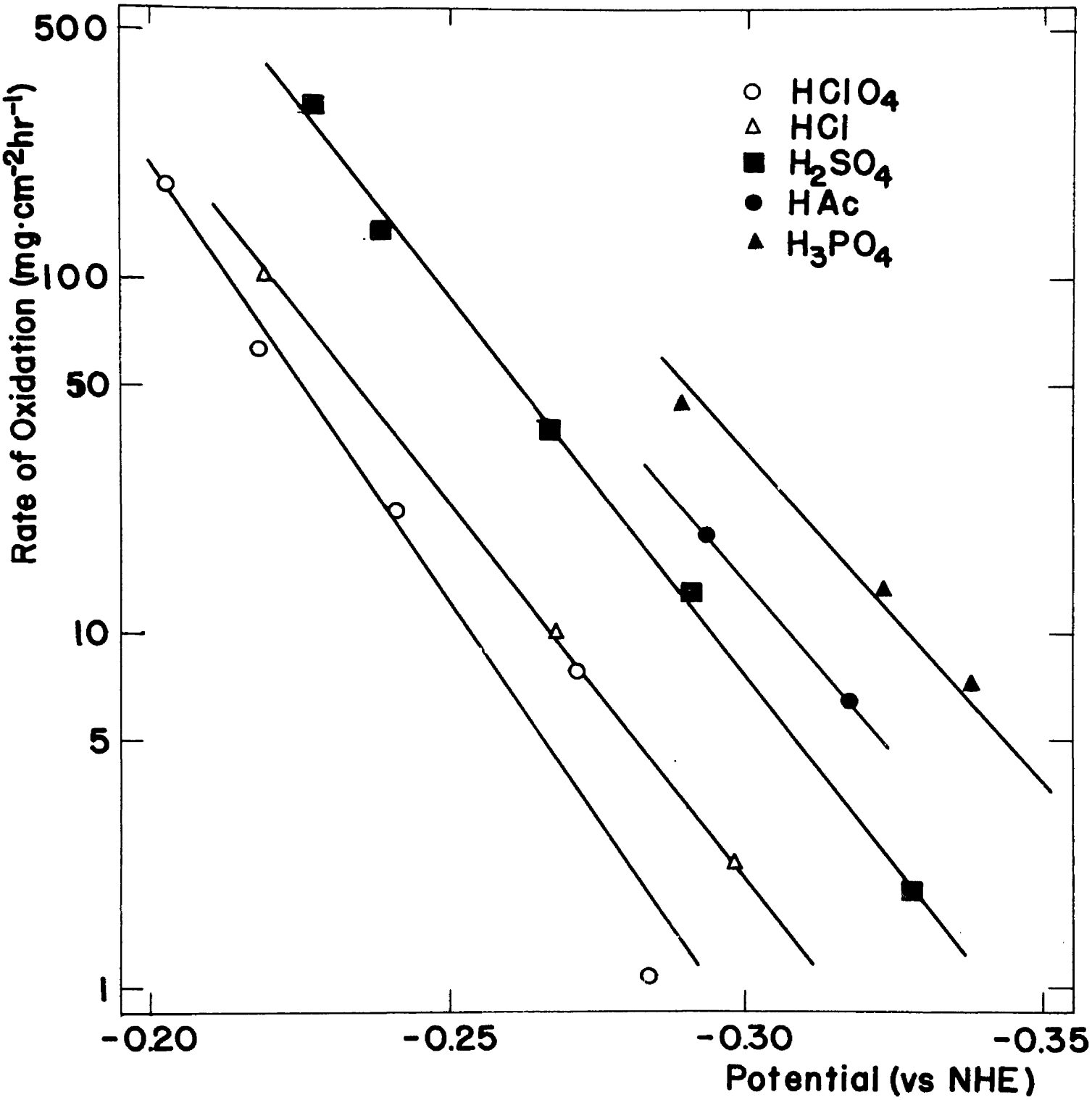

Figure 13. Influence of the anion on the rate of oxidation of iron.

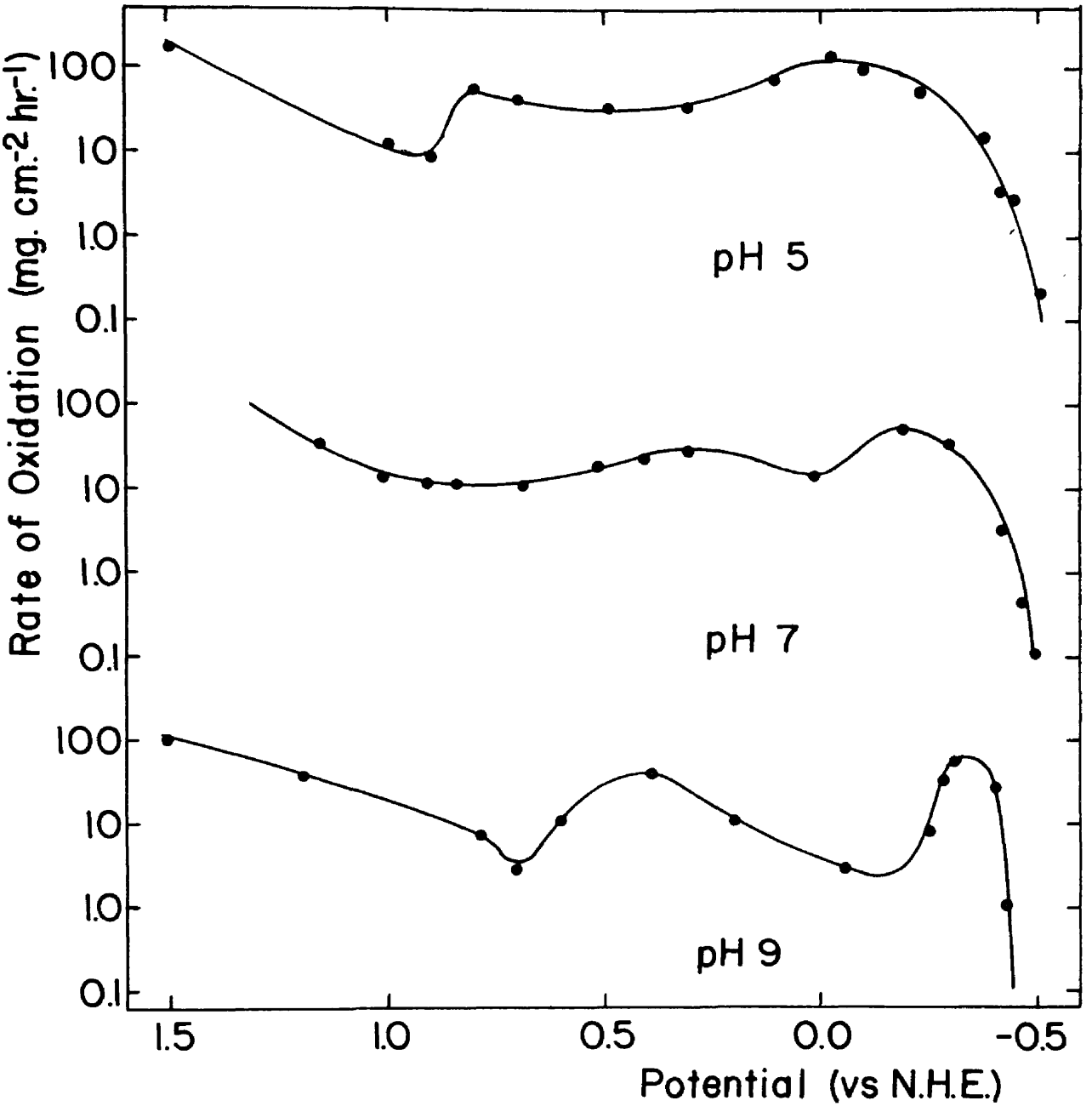

Figure 14. Influence of potential on the rate of oxidation of iron at three pH's.

are given in Appendix according to the list of tables given in Table IV. On the basis of these data one can construct a potential pH diagram showing lines of equal corrosion rates. Such a diagram is shown in Figure 15. The dotted lines shown in portions of the diagram correspond to rather uncertain experimental data. No rates of oxidation higher than 100 mg. $cm.^{-2}$ $hr.^{-1}$ were determined because these correspond to almost complete dissolution of the metallic specimens.

The above experimental results will be discussed in the light of the equilibrium potential-pH diagram which is shown in Figure 16. The characteristic features and the construction of such a diagram are discussed in the literature, and, consequently, only a few additional comments will be made. The diagram of Figure 16 represents the conditions of equilibrium between the various species shown. For example, the heavy horizontal line intersecting the ordinate axis at -0.44 volt represents the equilibrium between iron and ferrous ion for a unit activity of the latter species. The indica on each line are the logarithm of the concentration of the soluble species (activity coefficients are assumed to be equal to unity). Figure 16 shows that iron is thermodynamically stable in the lower part of the diagram. As the potential is made more anodic, iron is oxidized with the formation of ferrous ion, ferrous hydroxide and hypoferrite ion, depending upon the pH of the solution. As the potential is made still more anodic the ferric ion

TABLE IV

GUIDE TO TABLES OF DATA

FOR THE STUDY OF IRON

pH	Table[12]
I	VII
II	VII
13	VIII
14	VIII

[12] Tables VII and VIII are in the appendix.

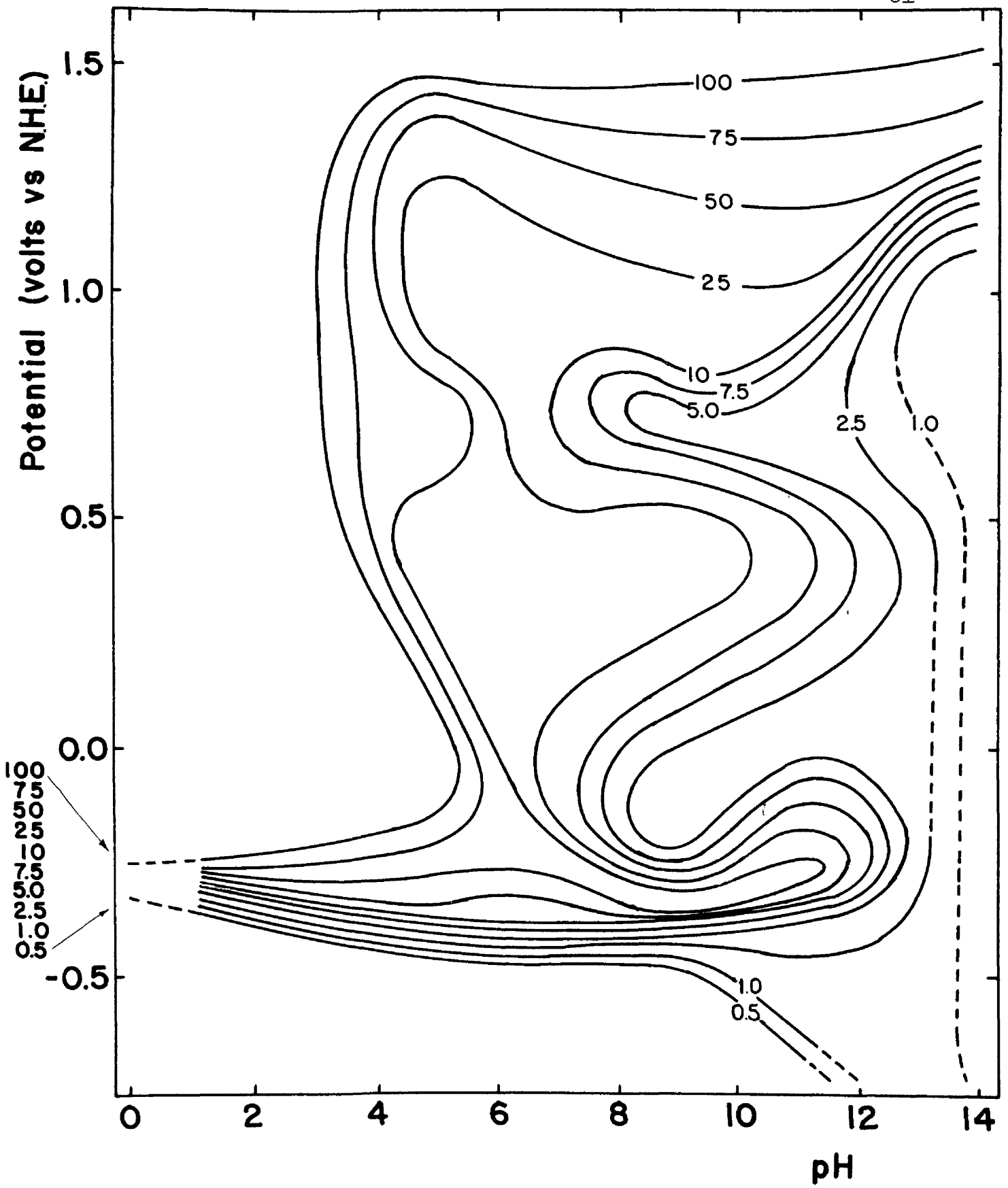

Figure 15. "Potential-pH-Oxidation Rate" diagram for iron. (The number on each line is the rate of oxidation in mg. cm.$^{-2}$ hr.$^{-1}$.)

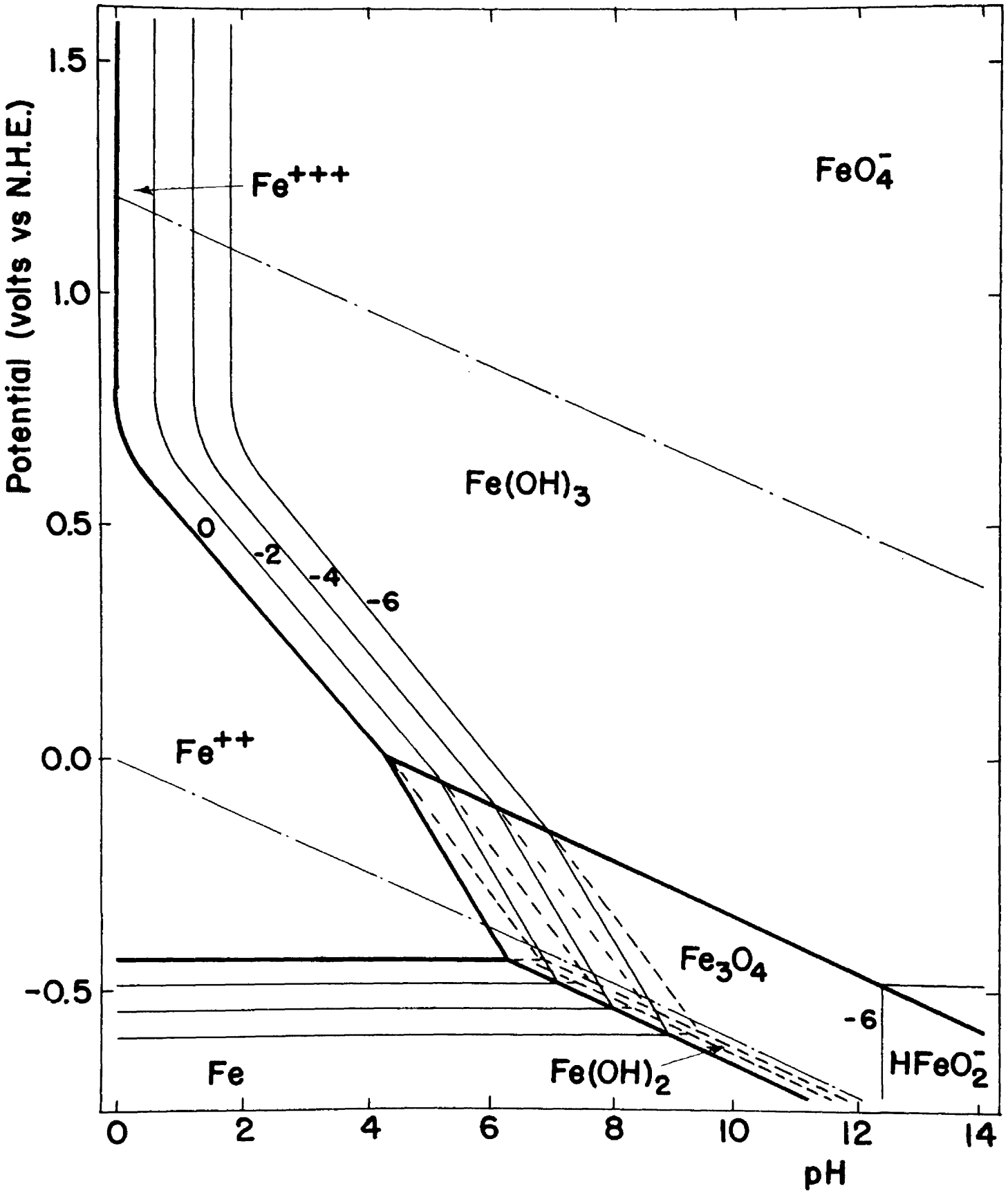

Figure 16. Potential-pH diagram for iron.

and its corresponding compounds are formed. More powerful oxidation brings the iron to the hexavalent state (FeO_4^{--}) in very alkaline solutions. Several species, such as FeO_2^-, were not taken into account, but the present diagram is adequate in this study. It should be pointed out that the boundaries of the area of the diagram in which magnetite Fe_3O_4 is the predominate species are rather uncertain, because the standard free energy of the formation of this compound is not known accurately (variation resulting from hydration, etc.).

It is seen from Figure 15 that the rate of oxidation was very low in the lower portion of the diagram. This can be readily understood, since this area corresponds to the thermodynamic stability of metallic iron as one can ascertain from Figure 16. As the potential was made more anodic, in the acid region (pH $<$ 4 - 5), the rate of oxidation increased with the formation of soluble ferrous ion. At potentials more anodic than approximately -0.25 volt, the rate of oxidation was too high to be measured by the procedure used in this investigation. The rate of oxidation in neutral and alkaline solutions first increased with more anodic potentials, and then decreased. This resulted in the "finger like" area extending across the base of the diagram. The probable explanation for this effect is as follows: as the potential is made more anodic, iron is oxidized to ferrous hydroxide; at more anodic potentials the oxidation proceeds to the magnetite which protects the metal more

effectively than ferrous hydroxide. It was indeed observed experimentally that the specimens in this range of potentials and pH's were coated with a dark blue film of magnetite. Magnetite is stable over a large area of this potential-pH diagram, and this is reflected in the diagram of Figure 15. (compare Figure 15 and Figure 16.) Oxidation of magnetite to ferric hydroxide is observed at sufficiently anodic potentials (approximately 0.6 volts vs. N. H. E.), and this process results in a decrease in the oxidation rate. Finally, at very anodic potentials oxygen is evolved. This results in an increase in oxidation rate, because of the pitting of the electrode. The localized oxidation probably results from variations of the overvoltage for the oxygen evolution from one point of the electrode to another. Thus, oxygen is evolved on a small area of the electrode, and the film of oxide protecting (more or less) the metal in these areas is disrupted. At anodic potentials of the order of 1.5 volts (vs. N. H. E.), the protective action of the film of ferric hydroxide is rather limited, and the rates of oxidation are accordingly rather high.

In the very alkaline range (pH of the order of 14), there is rapid increase in oxidation rate at potentials more anodic than 1 volt. This effect may be caused by the formation of a soluble species, i.e., ferrate ion FeO_4^{--}.

It can be seen by comparing Figure 15 and Figure 16 that there is a striking parallelism between the equilibrium diagram and the diagram showing the variations of the

oxidation rate with potential and pH. There is sometimes a shift in potential, but the essential features of both diagrams are similar.

To aid in the visualization of the results summarized in Figure 15, a three dimensional model of this diagram was constructed. A photograph of this model is shown in Figure 17.

II - THE ELECTROLYTIC OXIDATION OF TIN

Rates of corrosion for tin at various potentials and pH's are given in Appendix according to the information given in Table V. The corresponding potential-pH diagram with lines of equal corrosion rates is shown in Figure 18. This diagram will be discussed in the light of the equilibrium diagram of Figure 19 (40).

The high oxidation rates at low pH's (pH 2) and at potentials more anodic than 0.2 correspond to the formation of soluble species, i.e. stannous and/or stannic ion. In this region of the potential-pH diagram samples were observed to be coated with a black film. This film dissolved very slowly in the acid used to clean the specimen following electrolysis. Vaubel (45) made similar observations when he electrolyzed tin in hydrochloric acid. He believed it to be a modification of the metal. A similar black substance has been reported in connection with the corrosion of tin cans by acids. This substance proved to contain some SnO (32, 33).

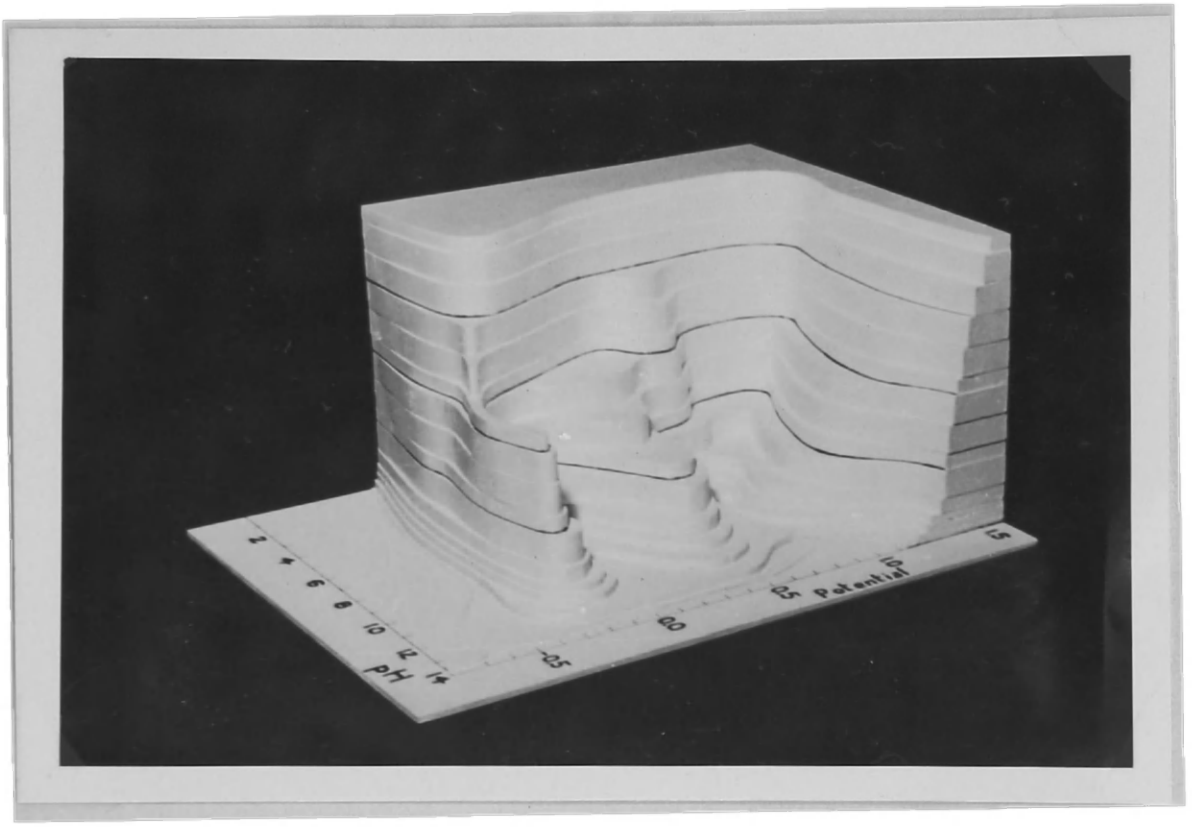

Figure 17. Three dimensional model of the Iron "Potential-pH-Oxidation-Rate" diagram.

TABLE V

GUIDE TO TABLES OF DATA

FOR THE STUDY OF TIN

pH	Table[13]
0	IX
1	IX
3	X
5	X
7	XI
9	XI
11	XII
13	XIII
14	XIII

[13] Tables IX through XIII are in the appendix.

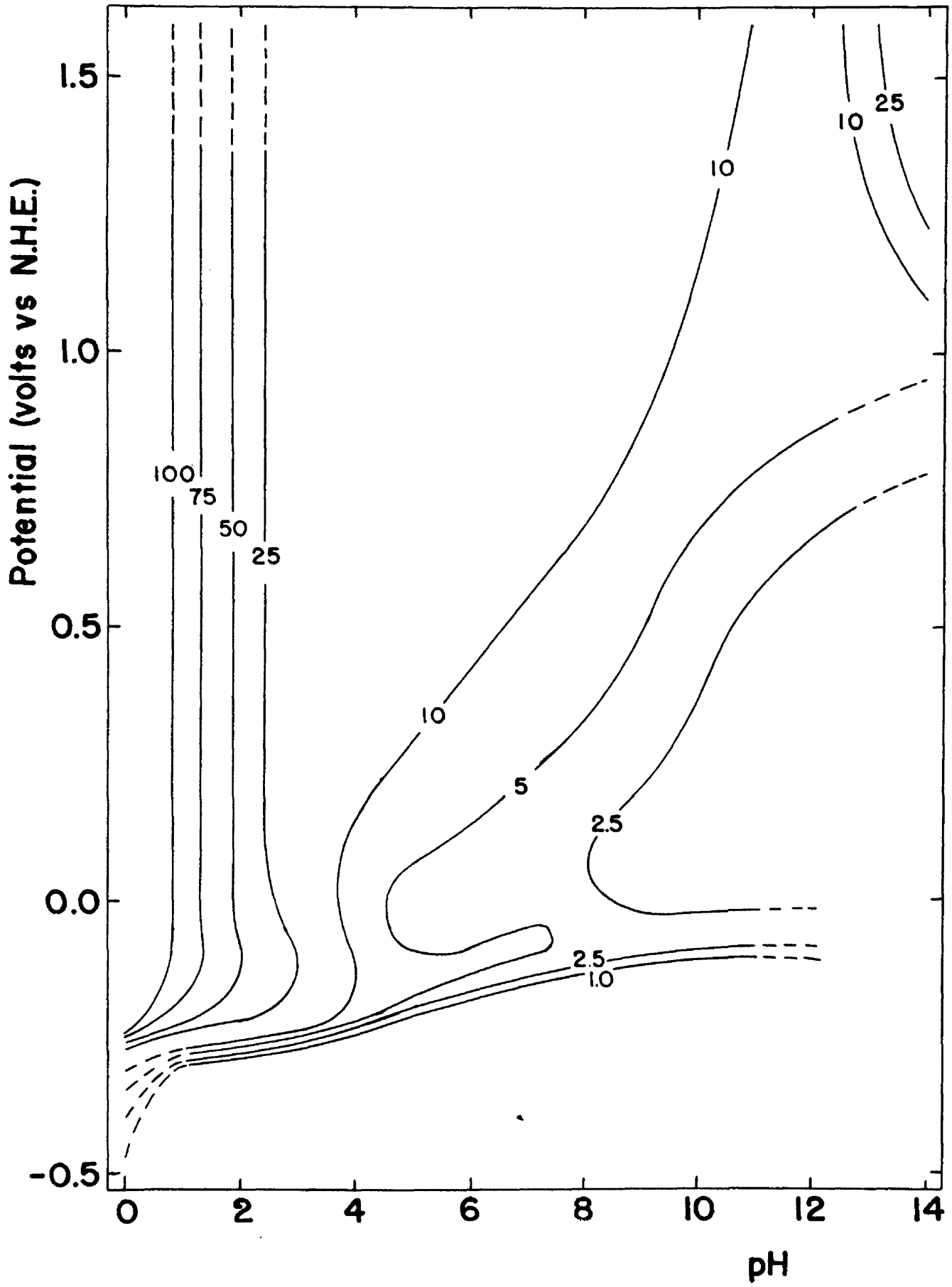

Figure 18. "Potential-pH-Oxidation Rate" diagram for tin. (The numbers on the lines are the rate of oxidation in mg. $cm.^{-2}$ $hr.^{-1}$.)

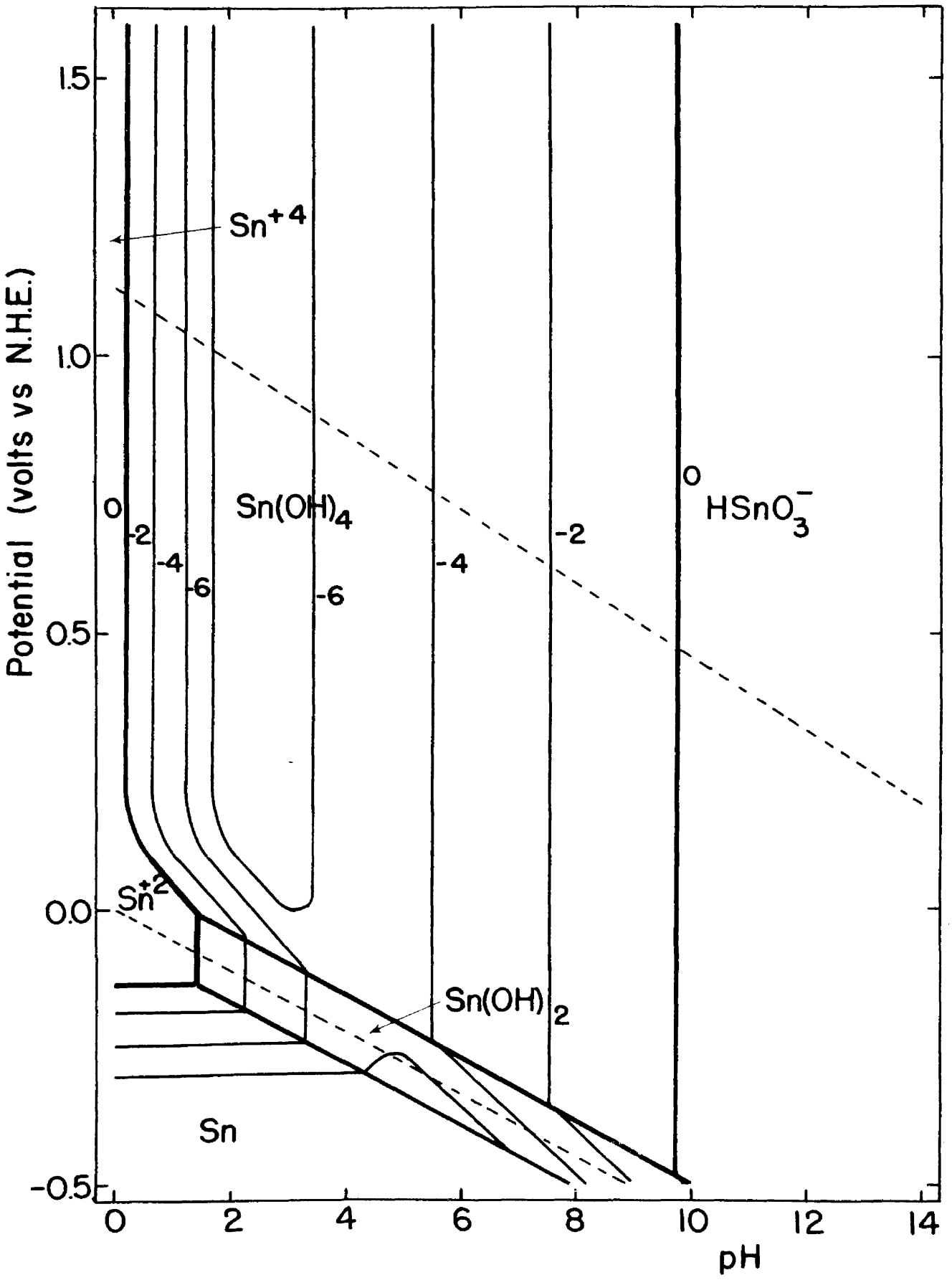

Figure 19. Potential-pH diagram for tin.

In the neutral pH range there was general passivation of the metal due to the formation of film of the solid hydroxides. In the lower part of the diagram there is an indication that in the case of tin, as for iron, the hydroxide of the lower valence state does not have the passivating effect shown by the corresponding higher valence compound.

Foerster and Dolch (18) observed that tin readily passivates in alkaline solution as the result of the formation of colloidal tin compound which is precipitated on the electrode. This prevents a diffusion of the stannic ions and the anode potential is raised to the value necessary for oxygen evolution. These observations correspond very closely to those results shown in Figure 18.

Dissolution of the tin was slow, until potentials sufficiently anodic for the evolution of oxygen were reached. It is also possible that the dismutation of the $HSnO_3^-$ ion in the alkaline range may contribute to the observed passivation.

III - THE ELECTROLYTIC OXIDATION OF LEAD

Experimental rates of oxidation of lead are given in Appendix according to the information given in Table VI. The experimental results are summarized in the potential-pH diagram of Figure 20. The equilibrium diagram as available

TABLE VI

GUIDE TO TABLES OF DATA

FOR THE STUDY OF LEAD

pH	Table[14]
1	XIV
3	XIV
5	XIV
7	XV
9	XV
11	XVI
13	XVI
14	XVII

[14] Tables XIV through XVIII are in the appendix.

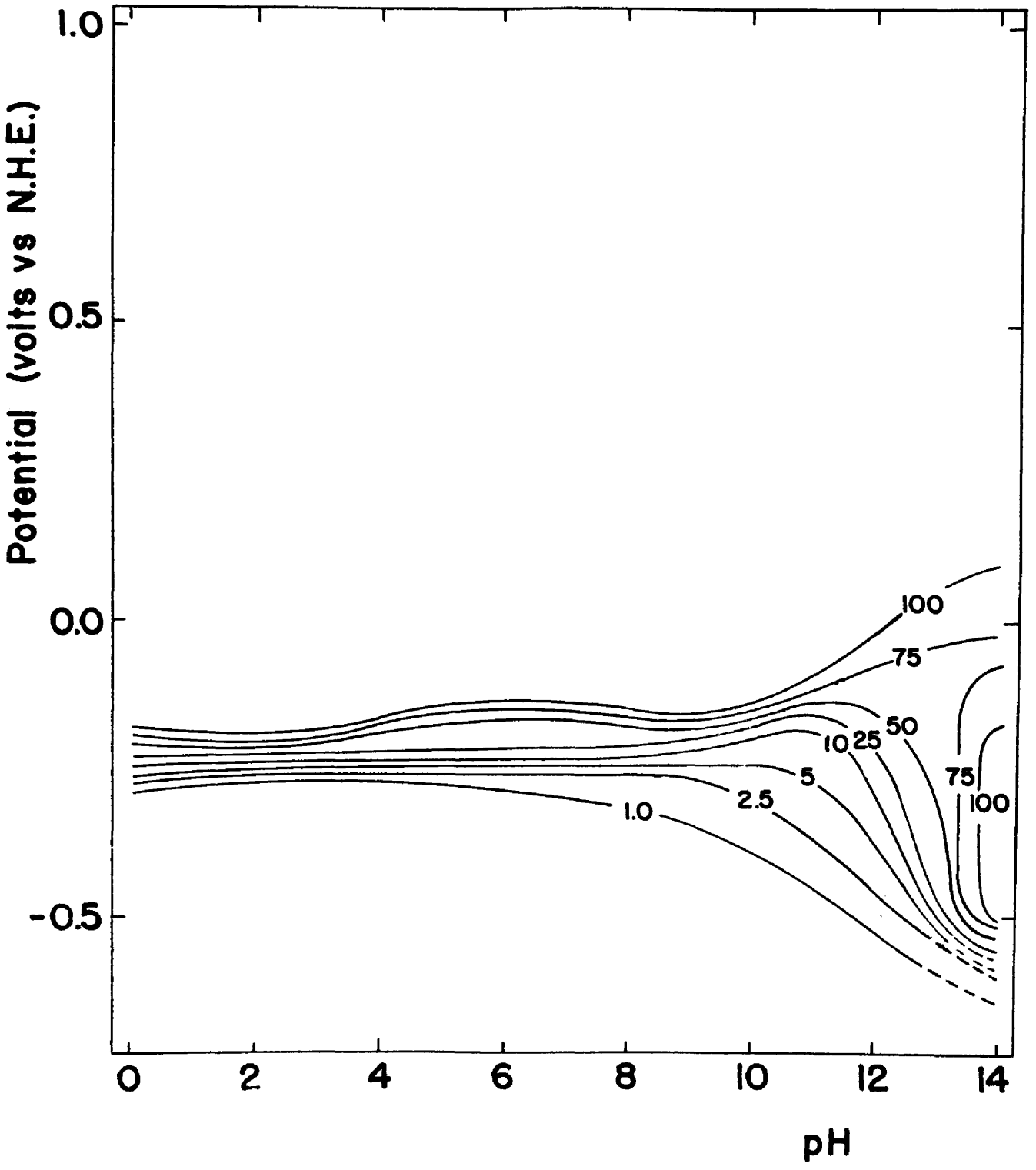

Figure 20. "Potential-pH-Oxidation Rate" diagram for lead. (The numbers on the lines are the rate of oxidation in mg. cm.$^{-2}$ hr.$^{-1}$.)

in the literature (14), is shown in Figure 21.[11] The lines of equal oxidation rates of the experimental diagram follow the general features of the equilibrium diagram. No passivation by the lead hydroxide is observed and consequently, the electro-chemical behavior of lead could not be explored at very anodic potentials in the present medium (perchlorate).

---

[11] It is to be noted that the diagram does not extend to high enough potentials to show the area of stability of the Pb^{+4} ion. The general area in which it is stable is shown by the arrow in the upper left hand corner of the diagram.

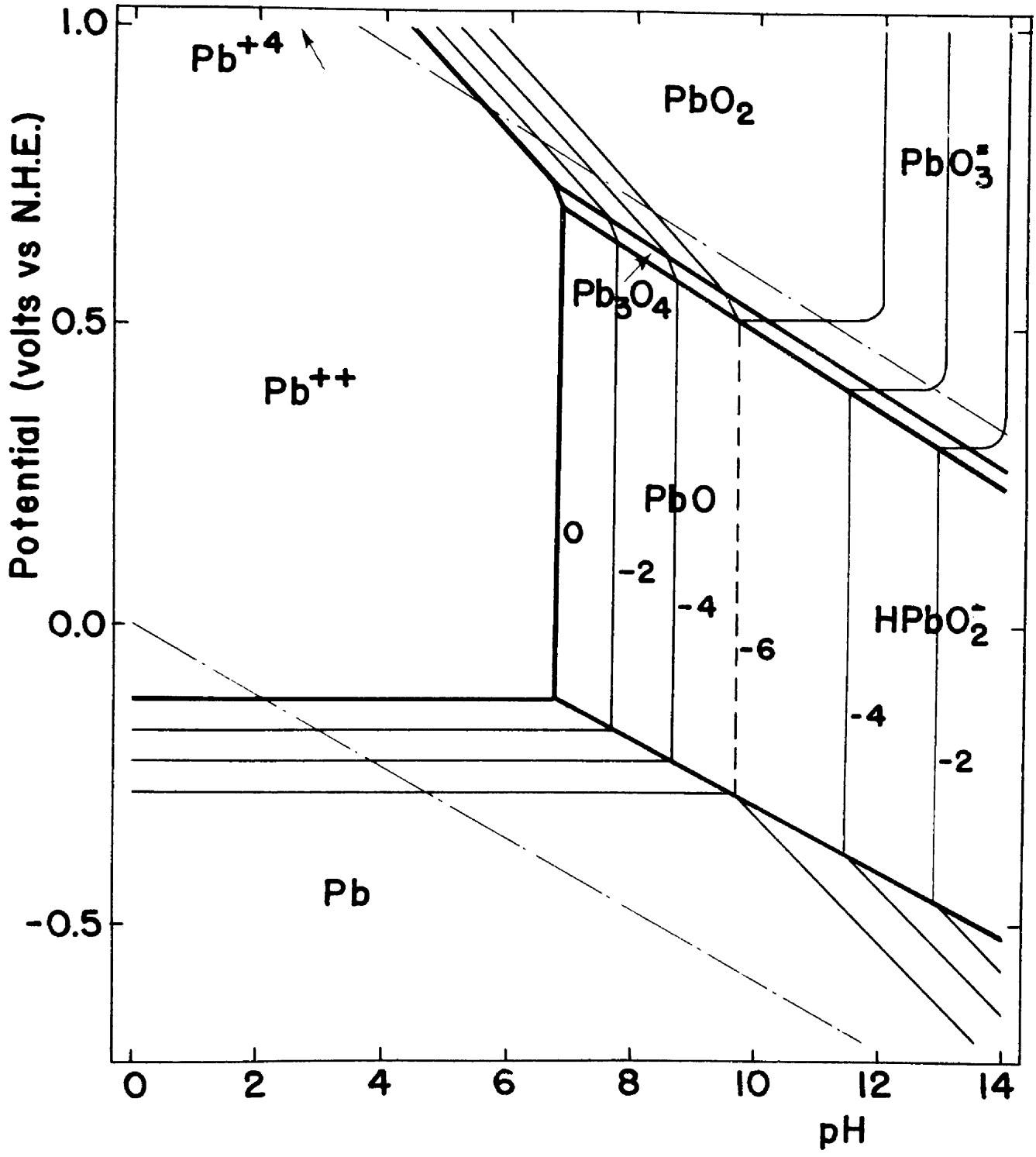

Figure 21. Potential-pH diagram for lead.

CONCLUSION

It can be concluded from the present investigation that there is a parallelism between the equilibrium potential-pH diagram for a given metal and the corresponding "potential-pH-oxidation rate" diagram. In areas of the equilibrium diagram in which a soluble species is predominant, the rates of oxidation are generally high. There are cases, however, in which this conclusion is not valid; for example, in the anodic oxidation of tin in alkaline solutions which proceeds at very low rates although high rates of oxidation would be predicted from the potential-pH diagram. In areas of the equilibrium diagram in which an insoluble species is predominant, rates of oxidation depend entirely on the nature of the film formed at the surface of the metal. For example, ferrous hydroxide gives very little protection to the metal, whereas ferric hydroxide is more efficient in that respect. Great caution should be exerted in predicting the electrochemical behavior of metals from equilibrium potential-pH diagrams, although it should be emphasized that these diagrams can be very useful in the interpretation of experimental rates of oxidation. The case of iron is typical from this point of view.

SELECTED BIBLIOGRAPHY

(1) Adams, T. J. Thesis, Studies in Polarography, Louisiana State University, 1952.

(2) Baxendale, J. E., Evans, M. E., and Park, G. S., "The Mechanism and Kinetics of the Initiation of Polymerization by Systems Containing Hydrogen Peroxide," Trans. Faraday Soc., 42, 155 (1946).

(3) Bircumshaw, L. L. and Riddiford, A. C., "Transport Control in Heterogeneous Reactions," Quarterly Reviews, VI, 157 (1952).

(4) Brdicka, R. and Trupp, C., "Polarographische Untersuchungen uber Blut Farbstoffe und ihre Derivate," Biochem. Z., 289, 301 (1936).

(5) Brdicka R. and Wiesner, K., "Polarographic Determination of the Rate of the Reaction between Ferrohem and Hydrogen Peroxide," Collection Czechoslov. Chem. Communs., 12, 39 (1947).

(6) Carslaw, H. S. and Jaeger, J. C., Conduction of Heat in Solids, Oxford, Oxford University Press, 1947. p. 57.

(7) Charlot, G., Theorie et Methode Nouvelle D'Analyse Qualitative, Third Edition. Paris, Wasson, 1949.

(8) Churchill, R. V., Modern Operational Mathematics in Engineering, New York, McGraw-Hill Book Co., Inc., 1944.

(9) Clark, W. M., The Determination of Hydrogen Ion, Third Edition. Baltimore, Williams and Wilkins, 1928. p. 387.

(10) Delahay, P., "A Polarographic Method for the Indirect Determination of Polarization Curves for Oxygen Reduction on Various Metals," J. Electrochem. Soc., 97, 198, 205 (1950).

(11) Delahay, P., "Theory of Polarographic Currents Controlled by Rate of Reaction and by Diffusion," J. Amer. Chem. Soc., 73, 4944 (1951).

(12) Delahay, P. and Adams, T. J., "Polarographic Study of the Kinetics of Ionic Recombination and Comparison with Onsager's Theory," J. Amer. Chem. Soc., 74, 1437 (1952).

(13) Delahay, P., Pourbaix, M. and Van Rysselberghe, P., "Potential-pH Diagrams," J. Chem. Education, 27, 683 (1950).

(14) Delahay, P., Pourbaix, M., and Van Rysselberghe, P., "Potential-pH Diagram of Lead and Its Applications to the Study of Lead Corrosion and to the Lead Storage Battery," J. Electrochem. Soc., 98, 57 (1951).

(15) Delahay, P., Pourbaix, M., and Van Rysselberghe, P., Potential-pH Diagram of Silver," J. Electrochem. Soc., 98, 65 (1951).

(16) Delahay, P., Pourbaix, M., and Van Rysselberghe, P., "Potential-pH Diagram of Zinc and Its Applications to the Study of Zinc Corrosion," J. Electrochem. Soc., 98, 101 (1951).

(17) Delahay, P. and Strassner, J. E., "A Theory of Irreversible Polarographic Waves," J. Amer. Chem. Soc., 73, 5219 (1951).

(18) Foerster, F. and Dolch, M., "Uber Das Verhalten von Zinnanoden in Natronlauge," Z. Elektrochem., 16, 599 (1910).

(19) Glasstone, S., Laidler, K. J., and Eyring, H., The Theory of Rate Processes, New York, McGraw-Hill Book Co., Inc., 1941, pp. 584-587.

(20) Griess, J. C., Jr. and Rogers, L. B., "Electroseparation of Traces of Silver from Palladium," J. Electrochem. Soc., 95, 129 (1949).

(21) Halser, F., "Uber die Elektrische Reduktion von Nichtelektrolyten," Z. Physical Chem., 32, 193 (1900).

(22) Hickling, A., "Studies in Electrode Polarization- Part IV- The Automatic Control of the Potential of a Working Electrode," Trans. Faraday Soc., 38, 27 (1942).

(23) Ilkovic, D., "Polarographic Studies with the Dropping Mercury Cathode - Part XLIV - The Dependence of Limiting Currents on the Diffusion Constant, on the Rate of Dropping, and on the Size of Drops," Collection Czechoslov. Chem. Communs., 6, 498 (1934).

(24) Kirkpatrick, H. F. W., "Polarographic Study of Alkaloids," Quart. J. Pharm. Pharmacol., 18, 245, 338 (1946); 19, 8, 127, 526 (1946) 20, 87 (1947).

(25) Kolthoff, I. M. and Lingane, J. J., Polarography, New York, Inter-Science Publishers, Inc., 1941. pp. 405-420.

(26) Kolthoff, I. M. and Parry, E. P., "Catalytic Polarographic Waves of Hydrogen Peroxide I the Kinetic Wave for the Ferric Iron-Hydrogen Peroxide System," J. Amer. Chem. Soc., 73, 3718 (1951).

(27) Lamphere, R. W. and Rogers, L. B. "Instrument for Controlled-Potential Electrolysis," Anal. Chem., 22, 463 (1950).

(28) Lander, J. J., "Anodic Corrosion of Lead in Sulfuric Acid Solutions," J. Electrochem. Soc., 98, 213 (1951).

(29) Levich, B., "The Theory of Concentration Polarization," Acta Physicochim., U. R. S. S., 17, 257 (1942).

(30) Lingane, J. J., "Controlled Potential Electroanalysis," Anal. Chem. Acta, 2, 584 (1948).

_____., "Recent Applications of Controlled Potential Electrolysis," Faraday Soc. Disc., 1, 203 (1947).

(31) McKay, R. J. and Worthington, K., Corrosion Resistance of Metals and Alloys, New York, Reinhold Publishing Corp., 1936. p. 406.

(32) Mantell, C. L., Tin, Its Mining, Production, Technology and Applications, New York, Reinhold Publishing Corp., 1949. p. 450.

(33) Mantell, C. L. and Lincoln, E. S., "Corrosion of Tin Plate in Tin Cans," Can. Chem. and Met., 11, 29 (1927).

(34) Michaelis, L., Oxidation-Reduction Potentials, Philadelphia, Lippincott, 1930. p. 89.

(35) Miller, S. L. "Polarographic Currents from a Combination of Diffusion and Reaction," J. Amer. Chem. Soc., 74, 4130 (1952).

(36) Nernst, W., "Theorie der Reaktionsyeschwindigkeit in Heterogenen Systemen," Z. Physical Chem., 47, 52 (1904).

(37) Noyes, A. A. and Whitney, W. R., "Uber die Auflosungsgeschwindigkeit von festen Stoffen in ihren eigenen Losungen," Z. Physical Chem., 23, 689 (1897).

(38) Pierce, B. O., A Short Table of Integrals, New York, Ginn and Co., 1929. p. 120.

(39) Piontelli, R., "Influence de l'anion sur le comportement electrochimique des Metaux," Proceeding of the Second Meeting of the International Committee of Electrochemical Thermodynamics and Kinetics, Milan, Tamkurini, 1950. p. 185.

(40) Pourbaix, M., Thermodynamique des Solutions Aqueuses Diluees Representation Graphique du Role du pH et du Potential, Delft, Meinema, 1945. Also, Paris, Beranger, 1948. English Translation by J. N. Agar, London, Arnold, 1949.

(41) Rogers, L. B., "Electrodeposition Behavior of Traces of Silver, II, Effects of Electrode History and the Presence of Other Ions," J. Electrochem. Soc., 98, 447 (1951).

(42) Rogers, L. B., Krause, D. P., Griess, J. C., and Ehrlinger, D. B., "The Electrodeposition in Behavior of Traces of Silver," J. Electrochem. Soc., 95, 33 (1949).

(43) Strassner, J. E., Thesis, A Study of Polarographic Currents Controlled by Rate of Reaction and by Diffusion," Louisiana State University, 1952.

(44) Van Rysselberghe, P., Delahay, P., Gropp, A. H., McGee, J. M., and Williams, R. D., "Polarographic Observations on Percarbonic Acids and Percarbonates," J. Phys. Chem., 54, 754 (1950).

(45) Vaubel, W., "Zur Kenntnis des Zinn Wasserstoffs," Ber., 57, B, 515 (1924).

VITA

George L. Stiehl, Jr. was born November 29, 1923, in Oklahoma City, Oklahoma. He graduated in 1941 from Classen High School in that city. He entered Oklahoma City University in 1941 and was called to military service in 1943. He served in the Pacific theater of operations from July, 1944 to December, 1945. He re-entered Oklahoma City University in 1947 and received a Bachelor of Science degree in May, 1949. He enrolled in the graduate school of Louisiana State University in September, 1949, and received the degree of Master of Science in June, 1951. He is now a candidate for the degree of Doctor of Philosophy.

APPENDIX

TABLE VII

DATA FOR THE STUDY OF IRON

Loss of Weight at pH 1

(0.1 N H_2SO_4)

Electrode Potential (vs N.H.E.)	Loss of Weight in mg. $cm.^{-2}hr.^{-1}$
-0.3377	0.38
-0.3279	1.82
-0.3177	1.84
-0.2900	13.12
-0.2665	37.5
-0.2375	137.9
-0.2269	304.2

Loss of Weight at pH 11

(Automatic Control)

Electrode Potential (vs N.H.E.)	Loss of Weight in mg. $cm.^{-2}hr.^{-1}$
-0.7052	0.18
-0.4555	2.86
-0.3894	2.78
-0.3071	52.6
-0.1979	35.8
-0.1635	18.32
-0.1026	145.7
-0.0029	9.67
+0.0921	4.99
+0.2955	11.08
+0.5045	9.15
+0.6046	14.5
+0.7036	89.7
+0.9059	96.7
+1.0045	30.4
+1.2043	10.92

TABLE VIII

DATA FOR THE STUDY OF IRON

Loss of Weight at pH 13

(0.1 M NaOH)

(0.1 N Na_2SO_4)

Electrode Potential (vs N.H.E.)	Loss of Weight in mg. $cm.^{-2} hr.^{-1}$
+0.8846	0.36
+0.9931	0.62
+1.1014	2.85
+1.2145	15.16
+1.2723	78.5

Loss of Weight at pH 14

(1.0 M NaOH)

(0.1 N Na_2SO_4)

Electrode Potential (vs N.H.E.)	Loss of Weight in mg. $cm.^{-2} hr.^{-1}$
-1.0630	0.73
+0.8828	0.41
+1.0323	1.65
+1.1336	5.83
+1.2087	12.16

TABLE IX

DATA FOR THE STUDY OF TIN

Loss of Weight at pH 0

(1 N H_2SO_4)

Electrode Potential (vs N.H.E.)	Loss of Weight in mg. $cm.^{-2}hr.^{-1}$
-0.7265	0.25
-0.6276	2.82
-0.3059	14.67
-0.2875	20.1
-0.2664	23.5
-0.2358	too high to measure

Loss of Weight at pH 1

(0.1 N H_2SO_4)

Electrode Potential (vs N.H.E.)	Loss of Weight in mg. $cm.^{-2}hr.^{-1}$
-0.3091	0.60
-0.2657	3.62
-0.2482	13.28
-0.2120	42.4
-0.1108	72.2
-0.0054	64.0
+0.0916	67.3
+0.1937	65.5
+0.2951	59.5
+0.4076	70.9
+0.5079	79.7
+0.7121	95.8
+0.8145	105.4
+1.0201	62.0
+1.2222	86.4
+1.5226	83.5
+1.9289	72.5

TABLE X

DATE FOR THE STUDY OF TIN

Loss of Weight at pH 3

(Automatic Control)

Electrode Potential (vs N.H.E.)	Loss of Weight in mg. $cm.^{-2} hr.^{-1}$
-0.2364	1.95
-0.2031	25.9
-0.1097	15.6
-0.0110	7.95
+0.0924	12.91
+0.1949	11.4
+0.4075	21.5
+0.6105	17.4
+0.8130	26.9
+1.0184	50.5
+1.2143	26.4
+1.4181	16.1
+1.6315	64.5

Loss of Weight at pH 5

(Automatic Control)

Electrode Potential (vs N.H.E.)	Loss of Weight in mg. $cm.^{-2} hr.^{-1}$
-0.2121	0.50
-0.1755	2.35
-0.1110	2.35
-0.0098	14.1
+0.1945	19.3
+0.4079	18.9
+0.6120	11.1
+0.7120	34.3
+0.8140	24.3
+1.0129	17.9
+1.2202	13.7
+1.4210	14.2
+1.6233	14.0
+1.8171	9.0

TABLE XI

DATA FOR THE STUDY OF TIN

Loss of Weight at pH 7

(Automatic Control)

Electrode Potential (vs N.H.E.)	Loss of Weight in mg. $cm.^{-2}hr.^{-1}$
-0.1645	0.75
-0.1092	4.20
-0.0594	0.85
-0.0069	2.20
+0.1945	5.05
+0.4056	18.5
+0.5595	11.2
+0.6099	7.75
+0.8156	47.7
+1.0137	17.1
+1.2176	17.5
+1.4073	11.6
+1.6145	6.60
+1.7346	53.6
+1.8420	28.0

Loss of Weight at pH 9

(Automatic Control)

Electrode Potential (vs N.H.E.)	Loss of Weight in mg. $cm.^{-2}hr.^{-1}$
-0.1120	0.97
-0.0091	1.00
+0.0928	3.47
+0.1942	12.55
+0.2969	7.15
+0.4078	5.50
+0.6072	6.90
+0.7121	8.39
+0.8158	28.15
+0.9159	2.74
+1.0156	7.95
+1.2180	11.8
+1.4211	10.6
+1.5273	6.36
+1.6205	39.5
+1.7304	96.4
+1.8239	17.4

TABLE XII

DATA FOR THE STUDY OF TIN

Loss of Weight at pH 11

(Automatic Control)

Electrode Potential (vs N.H.E.)	Loss of Weight in mg. $cm.^{-2} hr.^{-1}$
-0.1314	0.49
-0.1067	1.15
-0.0623	2.89
+0.0287	1.10
+0.0935	1.50
+0.1946	2.85
+0.2969	4.80
+0.4076	2.75
+0.6087	2.55
+0.7130	4.15
+0.8124	11.3
+1.0135	13.7
+1.2209	21.5
+1.4134	21.9
+1.6228	12.7
+1.8336	8.20

TABLE XIII

DATA FOR THE STUDY OF TIN

Loss of Weight at pH 13

(0.1 M NaOH)

(0.1 N Na_2SO_4)

Electrode Potential (vs N.H.E.)	Loss of Weight in mg. $cm.^{-2} hr.^{-1}$
+1.4844	19.5
+1.6289	11.5
+1.8249	9.50

Loss of Weight at pH 14

(1.0 M NaOH)

(0.1 N Na_2SO_4)

Electrode Potential (vs N.H.E.)	Loss of Weight in mg. $cm.^{-2} hr.^{-1}$
+1.2248	26.5
+1.4291	26.5
+1.6423	35.5
+1.8364	20.5
+1.8437	28.5

TABLE XIV

DATA FOR THE STUDY OF LEAD

Loss of Weight at pH 1

(0.1 M $HClO_4$)

Electrode Potential (vs N.H.E.)	Loss of Weight in mg. $cm.^{-2} hr.^{-1}$
-0.3155	0.40
-0.2560	4.95
-0.2150	36.1
-0.1638	232.5

Loss of Weight at pH 3

(Automatic Control)

Electrode Potential (vs N.H.E.)	Loss of Weight in mg. $cm.^{-2} hr.^{-1}$
-0.2961	0.36
-0.2660	2.80
-0.2363	5.30
-0.2265	10.9
-0.2163	34.5

Loss of Weight at pH 5

(Automatic Control)

Electrode Potential (vs N.H.E.)	Loss of Weight in mg. $cm.^{-2} hr.^{-1}$
-0.3133	1.35
-0.2166	5.15
-0.1599	22.7
-0.1142	197.9

TABLE XV

DATA FOR THE STUDY OF LEAD

Loss of Weight at pH 7

(Automatic Control)

Electrode Potential (vs N.H.E.)	Loss of Weight in mg. $cm.^{-2} hr.^{-1}$
-0.3665	1.10
-0.2739	1.10
-0.2178	7.15
-0.1100	89.4

Loss of Weight at pH 9

(Automatic Control)

Electrode Potential (vs N.H.E.)	Loss of Weight in mg. $cm.^{-2} hr.^{-1}$
-0.3637	0.65
-0.3035	1.65
-0.2211	3.45
-0.1600	78.8
-0.0551	244.6

TABLE XVI

DATA FOR THE STUDY OF LEAD

Loss of Weight at pH 11

(Automatic Control)

Electrode Potential (vs N.H.E.)	Loss of Weight in mg. $cm.^{-2}hr.^{-1}$
-0.3133	0.90
-0.2507	1.42
-0.2199	6.10
-0.1646	14.3
-0.1490	55.0
-0.1103	163.7
-0.1096	189.0
-0.0617	167.0

Loss of Weight at pH 13

(0.1 M NaOH)

(0.1 M $NaClO_4$)

Electrode Potential (vs N.H.E.)	Loss of Weight in mg. $cm.^{-2}hr.^{-1}$
-0.5646	1.00
-0.5123	17.4
-0.4092	17.1
-0.3640	11.7
-0.3100	16.4
-0.2485	15.5
-0.2134	13.5
-0.1095	88.6
-0.0066	81.0
+0.0945	105.0

EXAMINATION AND THESIS REPORT

Candidate: George L. Stiehl

Major Field: Chemistry

Title of Thesis: Studies of the Kinetics of Electrode Processes

Approved:

Paul Delahay
Major Professor and Chairman

Richard J. Russell
Dean of the Graduate School

EXAMINING COMMITTEE:

Vincent E. Parker

O. A. Nance

H. C. Edwards

Eugene W. Berg

Stanley Bastkin

Maurice M. Nick

Date of Examination:

May 5, 1953